Major Depressive Disorder Is Associated With Abnormal Interoceptive Activity and Functional Connectivity in the Insula

Jason A. Avery, Wayne C. Drevets, Scott E. Moseman, Jerzy Bodurka, Joel C. Barcalow, and W. Kyle Simmons

Background: Somatic complaints and altered interoceptive awareness are common features in the clinical presentation of major depressive disorder (MDD). Recently, neurobiological evidence has accumulated demonstrating that the insula is one of the primary cortical structures underlying interoceptive awareness. Abnormal interoceptive representation within the insula may thus contribute to the pathophysiology and symptomatology of MDD.

Methods: We compared functional magnetic resonance imaging blood oxygenation level-dependent responses between 20 unmedicated adults with MDD and 20 healthy control participants during a task requiring attention to visceral interoceptive sensations and also assessed the relationship of this blood oxygenation level-dependent response to depression severity, as rated using the Hamilton Depression Rating Scale. Additionally, we examined between-group differences in insula resting-state functional connectivity and its relationship to Hamilton Depression Rating Scale ratings of depression severity.

Results: Relative to the healthy control subjects, unmedicated MDD subjects exhibited decreased activity bilaterally in the dorsal midinsula cortex (dmlC) during interoception. Activity within the insula during the interoceptive attention task was negatively correlated with both depression severity and somatic symptom severity in depressed subjects. Major depressive disorder also was associated with greater resting-state functional connectivity between the dmlC and limbic brain regions implicated previously in MDD, including the amygdala, subgenual prefrontal cortex, and orbitofrontal cortex. Moreover, functional connectivity between these regions and the dmlC was positively correlated with depression severity.

Conclusions: Major depressive disorder and the somatic symptoms of depression are associated with abnormal interoceptive representation within the insula.

Key Words: Depression severity, fMRI, functional connectivity, insula, interoception, major depressive disorder

Some of the most pervasive symptoms of major depressive disorder (MDD) involve somatic disturbances and an altered sense of body awareness (1,2). In particular, multiple behavioral and psychophysiological studies have reported decreased heartbeat perception in individuals with MDD (3–8). Despite these findings, the role of interoception in mood disorders remains poorly understood. Influential theoretical accounts and accompanying empirical evidence suggest that emotion and decision making are grounded in the perception of interoceptive signals (9–11), which accords well with MDD patients' clinical reports of emotional dissociation (12). With the advent of theories stating that mood and anxiety disorders are fundamentally disorders of interoception (13), there is clearly a need to understand the neural bases of interoception and how

the function of interoception-related brain regions may be related to depressive symptoms.

A limited number of previous interoception studies in MDD.

A limited number of previous interoception studies in MDD have employed behavioral measures of heartbeat perception accuracy as the primary metric of interoceptive awareness, with varied results (4,5). Some studies reported decreased accuracy in depression, but these findings were either based on data from subclinical populations (6) or from populations with varied medication status (5,7,8), confounding the interpretation of their results in regard to an effect of major depression. In contrast, both clinical and subclinical levels of anxiety were associated with increased interoceptive accuracy (3,14), a finding that appears challenging to reconcile with the reports of decreased accuracy in depression, since depressive and anxiety symptoms occur concomitantly in most patients with MDD. Findings based on heartbeat perception accuracy are further complicated by the fact that healthy subjects often do not show reliable heartbeat perception accuracy (3). Consequently, the interpretation of interoceptive accuracy metrics is challenging. Importantly, the recent finding that heartbeat evoked potential is reduced in depressed subjects (7) suggests that, apart from differences in interoceptive accuracy, the neural basis underlying the interoceptive signal itself may be disturbed in depression.

In healthy humans, recent neuropsychological and functional neuroimaging studies have established a role for the insula in interoceptive awareness (15–18). The insula receives afferent projections from the vagus nerve via the nucleus of the solitary tract and the parvocellular portion of the ventroposteromedial nucleus of the thalamus that convey visceral information important for homeostatic regulation (19–21). Meta-analyses of human neuroimaging studies, which parcellated the insula among

From the Laureate Institute for Brain Research (JAA, WCD, SEM, JB, JCB, WKS); and Department of Biological Sciences (JAA), The University of Tulsa, Tulsa, Oklahoma; Johnson & Johnson, Inc. (WCD), New Brunswick, New Jersey; and Laureate Psychiatric Clinics and Hospital (SEM); College of Engineering (JBo), The University of Oklahoma; and Faculty of Community Medicine (WKS), The University of Tulsa, Tulsa, Oklahoma

Address correspondence to William Kyle Simmons, Ph.D., Laureate Institute for Brain Research, 6655 South Yale Ave, Tulsa, OK 74136-3326; E-mail: wksimmons@gmail.com; wksimmons@laureateinstitute. org.

Received Jun 8, 2013; revised and accepted Nov 26, 2013.

various functional domains, have associated interoception with the activity of mid-insular cortex (22,23), a region that appears homeostatically sensitive (24). Likewise, hemodynamic activity increases in mid-insular cortex in human subjects performing tasks involving visceral interoceptive attention (15,25,26) or direct visceral stimulation (27,28). Notably, the mid-insula regions underlying interoception appear at least partially dissociable from dorsal and ventral anterior insula regions involved in cognitive and emotional processing, respectively (15), suggesting the hypothesis that multiple insula regions play distinct roles in the symptoms expressed in MDD, with somatic abnormalities observed in MDD conceivably resulting either from mood- and anxiety-related pathophysiology within the insula (29-32) or from abnormal visceral afferent input into this region (13).

The extensive structural and functional connectivity between the insula and other brain structures also provide indirect evidence for its role in MDD. The insula has strong functional connectivity to the medial prefrontal network of regions such as the subgenual prefrontal cortex (sgPFC) and other ventromedial prefrontal cortex regions that play major roles in visceromotor regulation and exhibit increased metabolism and resting-state functional connectivity in the depressed versus the nondepressed phases of MDD (15,33-35). The insula also shares substantial anatomical connections with the amygdala and orbitofrontal cortex (OFC) (36-38), regions that display molecular, histological, and functional abnormalities in MDD (33,39-41).

Given the reported interoceptive deficits in MDD and the insula's role in interoception, it is surprising that to date, no published study has directly demonstrated that depression is associated with abnormal insula function during interoception. If the neural circuitry involving viscerosensory regions of the insula underlies altered interoception in MDD, then we should observe the following: 1) During an interoceptive attention task, subjects with MDD will exhibit decreased hemodynamic response within the mid-insula. 2) The magnitude of the hemodynamic response in the insula during interoceptive attention will correlate with behavioral measures of depression severity and the severity of depressed subjects' self-reported somatic symptoms. 3) Given this region's extensive limbic connectivity (35,42), in MDD patients the mid-insula will exhibit increased functional connectivity to other limbic or paralimbic structures, particularly to the ventromedial prefrontal cortex and other regions implicated in depression, such as the amygdala and OFC. 4) The magnitude of functional connectivity to these regions will also relate to depression severity.

Methods and Materials

Participants

Forty right-handed, native English-speaking volunteers between the ages of 21 and 50 years participated in the study: 20 subjects with MDD (13 female subjects; mean [SD] age = 36 [9] years; range = 21-50 years) and 20 healthy control subjects (12 female subjects; mean [SD] age = 33 [7] years; range = 21-45 years). All subjects underwent clinical screening assessments, including a Structured Clinical Interview for DSM-IV Axis I Disorders (SCID-I) performed by Master's-level clinicians with experience in psychiatric diagnosis. In addition, for every subject, the SCID-I results were compared with those of psychiatric interviews performed by a research psychiatrist, with any discrepancies between the two assessments resolved before inclusion in the study. All depressed subjects met DSM-IV criteria for

MDD in a current major depressive episode. Depression severity was assessed using the 25-item Hamilton Depression Rating Scale (HDRS) (43). Anxiety severity was assessed using the Hamilton Anxiety Rating Scale (44).

Volunteers were excluded from participation if they had been exposed to psychotropic medications or other drugs likely to affect cerebral function or blood flow within 3 weeks (6 weeks for fluoxetine) or had manifested a major neurological or medical disorder, substance abuse, a past history of traumatic brain injury, or current pregnancy. Additionally, healthy control subjects were excluded for having met criteria for any Axis I psychiatric disorder on the SCID-I.

All subjects received compensation for their participation and provided written informed consent as approved by the University of Oklahoma Institutional Review Board.

Experimental Design

A high-resolution anatomical magnetic resonance imaging (MRI) scan was obtained for each subject, followed by a 450second resting-state blood oxygen level-dependent (BOLD)functional magnetic resonance imaging (fMRI) scan, during which the subject viewed a black fixation mark against a white background. During this time, they were asked to keep their eyes open, focus on the fixation mark, clear their mind, and not think of anything in particular.

After the resting-state scan, each subject completed three additional fMRI scans while undergoing the focused awareness task. Within each 9-minute, 10-second scan, they alternated between two experimental conditions, the interoceptive attention condition and the exteroceptive attention condition. During the interoceptive condition, the word HEART, STOMACH, or BLADDER was presented for 10 seconds in black font against a white background. During this time, subjects were instructed to focus attention on the intensity of the sensations experienced from that organ, such as heartbeat or stomach or bladder distension. Previous research has demonstrated that focal attention on a perceptual modality amplifies activity in brain regions underlying that modality (45-47). The interoceptive attention task used here capitalizes on this attentional spotlight effect by instructing participants to focus on their naturally occurring interoceptive sensations. We have previously demonstrated in healthy adults that this task is effective at mapping interoceptive regions in the insula (15). As an exteroceptive attention control condition, subjects fixated on the word TARGET, which randomly switched to the lowercase word (target) for a 500-millisecond duration during the 10-second exteroceptive task trial. Subjects were instructed to attend to the exteroceptive target and to count the number of times they saw the lowercase word during each 10-second trial. Following one half of the trials of each condition, the subjects were shown for 5 seconds a number line with values from 1 to 7 and asked to indicate via a magnetic resonance compatible scroll wheel either the intensity of the sensations (with 1 indicating no sensation and 7 indicating an extremely strong sensation) or the number of targets perceived in the preceding trial. These ratings were included to help ensure that subjects remained attentive to the task. After receiving verbal instructions, all subjects practiced the interoceptive and exteroceptive tasks before performing them in the scanner, were observed to make stimulus intensity responses, and finally were asked to indicate whether they had any remaining questions about the task demands.

For additional imaging task details, see Supplemental Methods in Supplement 1.

Data Acquisition

Functional and structural magnetic resonance images were collected using a General Electric Discovery MR750 whole-body 3-Tesla MRI scanner (GE Healthcare, Milwaukee, Wisconsin), using a scalable 32-channel digital MRI receiver capable of performing massively parallel fMRI. A brain-dedicated receive-only 32-element coil array (Nova Medical Inc., Wilmington, Massachusetts), optimized for parallel imaging, was used for MRI signal reception. A single-shot gradient-recalled echo-planar imaging sequence with sensitivity encoding depicting BOLD contrast was used for functional scans (see Supplemental Methods in Supplement 1 for detailed scan parameters). Simultaneous physiological pulse oximetry and respiration waveform recordings were collected for each fMRI run. The pulse oximetry readings were used to calculate heart rate during functional scans (see Supplemental Methods in Supplement 1).

Data Preprocessing and Subject-Level Statistical Analyses

Functional image preprocessing was performed using AFNI (http://afni.nimh.nih.gov/afni), as detailed in Supplemental Methods in Supplement 1. Each subject's data from the focused awareness task were analyzed using a multiple linear regression model.

Group Analyses

A whole-brain voxel-wise analysis was conducted to examine group differences in heartbeat interoceptive attention. The beta values derived from the contrast of heartbeat interoception versus the exteroceptive control condition, which indicate the mean percent signal change during interoceptive attention relative to exteroception, were extracted for each subject. These values were then included in a two-sample random effects *t* test.

Additionally, the HDRS scores of the depressed subjects were used to conduct a whole-brain voxelwise correlation analysis examining the relationship between heartbeat interoceptive attention and depression severity. Both analyses were performed using the AFNI program 3dttest++ and subsequently corrected for multiple comparisons at p < .05 (see Supplemental Methods in Supplement 1 for details).

Region of Interest Analyses

Using the dorsal mid-insula cortex (dmIC) clusters identified in the voxel-wise analysis above (Figure 1), the average beta coefficients for stomach interoception versus exteroception and bladder interoception versus exteroception were extracted within these regions of interest (ROIs), to examine group differences in these modalities. The relationship between insular activation during interoceptive attention and behavioral measures of depression and anxiety was also examined by calculating the correlation between the beta values for heartbeat attention versus exteroception within the dmlC clusters and the depressed subjects' HDRS and Hamilton Anxiety Rating Scale scores, respectively. Following this, post hoc analyses were conducted to further specify this relationship using the HDRS subscales as defined by Cleary and Guy (48). As we were primarily interested in the relationship of these variables and activity within these regions, these analyses were performed in an external statistical analysis suite.

Functional Connectivity Analyses

Because our primary interests were group differences in interoception-related brain activity and earlier studies demonstrated homeostatic sensitivity and selectivity for interoceptive attention in the dmlC (15,24), this region was used as the seed for

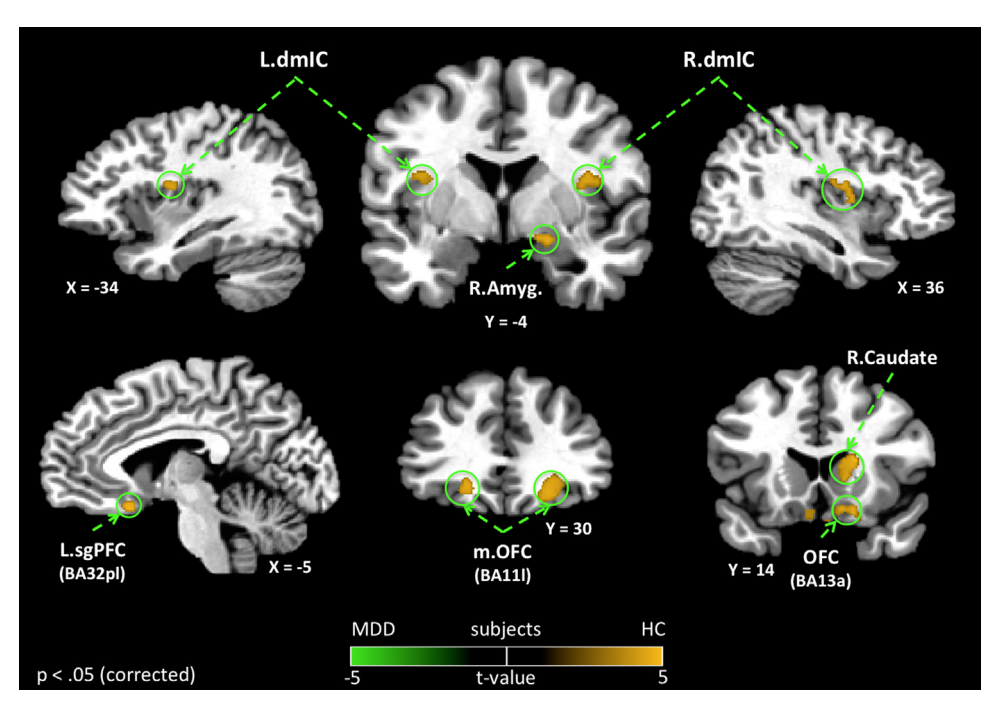


Figure 1. Group differences in heartbeat interoception. Depressed subjects (major depressive disorder [MDD]) exhibited decreased hemodynamic activity compared with healthy subjects (HC) within multiple brain regions during attention to heartbeat sensations. Group differences in heartbeat interoception were observed in bilateral dorsal mid-insula cortex (dmlC) and bilateral orbitofrontal cortex (OFC), as well as right amygdala (Amyg). Importantly, the group differences in heartbeat interoception within the insula were confined to regions of the dmlC that have been implicated in primary viscerosensory representation within the insula (15). All results shown were corrected for multiple comparisons at $p_{corrected} < .05$. BA, Brodmann area; L, left; m, medial; R, right; sgPFC, subgenual prefrontal cortex.

functional connectivity analyses of the resting-state BOLD image data. The seed time series from both dmIC ROIs (Figure 1) was used to identify brain regions that showed group differences in functional connectivity to the dmlC, as well as regions where dmIC resting-state functional connectivity was associated with behavioral measures of depression or anxiety. These analyses were performed using the AFNI program 3dttest++, and the resulting statistical maps were corrected for multiple comparisons at p < .05 (see Supplement 1 for details).

Results

The depression severity for the MDD group ranged from mild to severe (11 to 34), with a mean HDRS score of 23.1 (SD = 7.5; the demographic and clinical characteristics appear in Table 1 and Supplemental Results in Supplement 1). All of the MDD subjects were currently unmedicated, and none were currently undergoing psychotherapy. Eight of the MDD subjects were drug naive, and among those who previously had taken medications, the mean time free of psychotropic medications was 8.3 years (SD = 7.3years). Nine MDD subjects had secondary, comorbid anxiety disorders (social phobia n = 4, posttraumatic stress disorder n = 3, simple phobia n = 1, panic disorder n = 1); the performance and behavioral measures of these subjects did not differ from those without secondary comorbid anxiety diagnoses (Supplement 1).

Imaging Results

Group Differences in Activity During Interoceptive Attention. Voxelwise analysis revealed that depressed subjects exhibited decreased hemodynamic response during interoceptive attention to heartbeat sensations, specifically within the bilateral dmIC (Figure 1, Table 2). No other regions of the insula exhibited group differences in the hemodynamic response to heartbeat attention. Outside of the insula, depressed subjects exhibited significantly lower BOLD activity during heartbeat attention in multiple brain regions implicated in emotional, sensory, and reward processing, including the right amygdala, sgPFC (located

Table 1. Demographic and Clinical Characteristics of the Study Samples

| | НС | MDD | t ₃₈ | р |
|--|-----------|------------|-----------------|-------|
| Sample Size (n) | 20 | 20 | | |
| Age, Years (SD) | 33 (7) | 36 (9) | -1.3 | .20 |
| Gender | 12F | 13F | | |
| Body Mass Index (kg/m²) | 27.4 | 27.8 | 5 | .79 |
| Resting Heart Rate (bpm) | 66 (10) | 65 (8) | .5 | .63 |
| Task Heart Rate (bpm) ^a | 68 (8) | 66 (8) | .8 | .43 |
| HDRS, Mean (SD) | 1.2 (1.6) | 23.1 (7.5) | -12.0 | <.001 |
| HARS, Mean (SD) | 1.2 (1.9) | 17.0 (4.9) | -13.6 | <.001 |
| Age of Onset, Years (SD) | NA | 19 (10) | | |
| Illness Duration, Months (SD) ^b | NA | 61 (75) | | |
| Drug-Naïve (n/20) | NA | 8/20 | | |
| Currently Unmedicated | NA | 20/20 | | |
| Mean Duration Drug-Free, Months (SD) ^c | NA | 99 (87) | | |
| Comorbid Anxiety Disorder (n) | 0 | 9 | | |

F, female; HARS, Hamilton Anxiety Rating Scale; HC, healthy control subjects; HDRS, Hamilton Depression Rating Scale; MDD, major depressive disorder; MDE, major depressive episode; NA, not applicable.

Table 2. Brain Regions Exhibiting Differences in the Hemodynamic Response to Heartbeat Interoception Versus Exteroceptive Attention between Healthy and Depressed Subjects

| | Peak | Coordina | ates ^b | | Volume |
|----------------------------|------|----------|-------------------|-----------------|--------------------|
| Side/Location ^a | х | у | Z | t ₃₈ | (mm ³) |
| R lateral OFC (BA11I) | +24 | +29 | -8 | 4.01 | 1474 |
| R caudate | +18 | +17 | +14 | 4.46 | 1104 |
| L lateral OFC (BA11I) | -18 | +31 | -5 | 3.78 | 568 |
| L superior Parietal Lobule | -27 | -60 | +48 | 4.39 | 568 |
| R dmIC | +39 | -6 | +16 | 3.62 | 563 |
| R posterior OFC (BA13a) | +18 | +15 | -12 | 3.87 | 520 |
| L dmIC | -34 | -6 | +16 | 3.30 | 279 |
| R amygdala | +18 | -3 | -10 | 3.90 | 252 |
| L sgPFC (BA32pl) | -4 | +17 | -14 | 3.59 | 161 |

BA, Brodmann area; dmIC, dorsal mid-insula cortex; L, left; MDD, major depressive disorder; OFC, orbitofrontal cortex; R, right; sgPFC, subgenual

^aIn all cases, activity was greater in healthy subjects compared with the MDD group.

^bAll coordinates reported according to Talairach stereotaxic atlas (73). This format uses three numbers (x, y, z) to describe the distance from the anterior commissure. The x, y, z dimensions refer to right(+)-to-left(-), anterior(+)-to-posterior(-), and dorsal(+)-to-ventral(-), respectively.

in the putative prelimbic region corresponding to Brodmann area [BA] 32pl) (38,49), lateral OFC, posterior OFC (BA13a; located near the caudal part of the olfactory sulcus), and right caudate nucleus (Figure 1, Table 2).

A subsequent ROI analysis within the dmlC clusters revealed that depressed subjects also exhibited decreased BOLD activity for both stomach and bladder attention bilaterally in the dmIC (Figure S1 and Table S2 in Supplement 1; also see Figure S5 and Table S12 in Supplement 1 for results from voxelwise analyses of group differences during both stomach and bladder interoception).

The Relationship between Heartbeat Interoceptive Attention and Behavioral Symptom Severity. Using ROI analyses within the left dmlC cluster identified in the heartbeat attention contrast (Figure 1), a negative correlation between BOLD activity during heartbeat interoceptive attention and HDRS measures of depression severity was observed within the MDD group (left insula: r = -.44; p = .05; Figure 2, Table S3 in Supplement 1). Importantly, this appears to be largely attributable to the subjects' somatic-depressive complaints, as only the HDRS somatization subscale (48) exhibited a significant relationship with dmlC activity (r = -.53, p < .02; Figure 2, Table S4 in Supplement 1). None of the other HDRS subscales significantly related to dmlC activity (p > .5).

Additionally, voxelwise analyses outside the dmIC ROI revealed that depressed subjects exhibited a significant negative correlation between BOLD activity during heartbeat attention and HDRS measures of depression severity within left ventral anterior insular cortex and left ventral and dorsal mid-insula (Figure S2 and Table S5 in Supplement 1). Other regions exhibiting a negative correlation between depression severity and heartbeat interoception activity included the bilateral amygdala and left posterior OFC.

Functional Connectivity Results

Group Differences in Functional Connectivity to the dmlC. Depressed subjects exhibited significantly greater resting-state functional connectivity between the dmIC and multiple brain regions involved in affective and sensory processing (Figure 3, Table 3). Notably, bilateral dmIC exhibited significantly greater

^aHeart rate calculated during interoception tasks did not differ from average heart rate during the focused awareness task.

^bOf current MDE.

^cOf non-drug-naïve subjects.

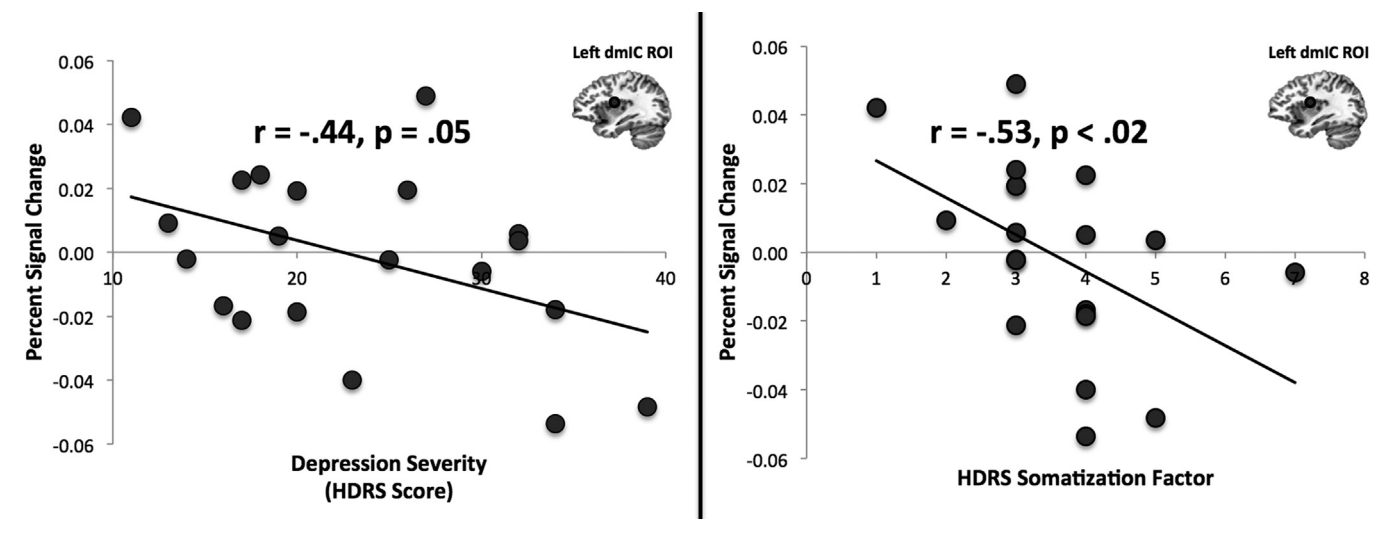


Figure 2. Dorsal mid-insula cortex (dmlC) activation during heartbeat interoception is correlated with depression severity and the severity of somatic symptoms. Within the left dmlC, which was identified in Figure 1, a significant negative correlation was observed between depressed subjects' hemodynamic response during heartbeat interoceptive attention vs. exteroception and scores on the Hamilton Depression Rating Scale (HDRS). A significant negative correlation was also observed between hemodynamic response and the HDRS somatization subscale (48) (see Supplemental Methods in Supplement 1). Values on the x axis indicate scores on the HDRS, which was administered before the functional magnetic resonance imaging scan. Values on the y axis are beta coefficients representing percent signal change during heartbeat interoception vs. exteroception within the left dmlC cluster from Figure 1. Circular regions of interest (ROIs) in left dmlC are for illustrative purposes only.

functional connectivity to the amygdala and medial OFC in depressed versus healthy subjects.

Functional Connectivity to the dmlC Is Associated with Depression Severity. Within the MDD group, depression severity,

as measured by the HDRS, was positively associated with functional connectivity between the dmlC and both the left amygdala and the medial OFC (Figure S2 and Table S5 in Supplement 1), regions that also exhibited increased dmlC functional connectivity

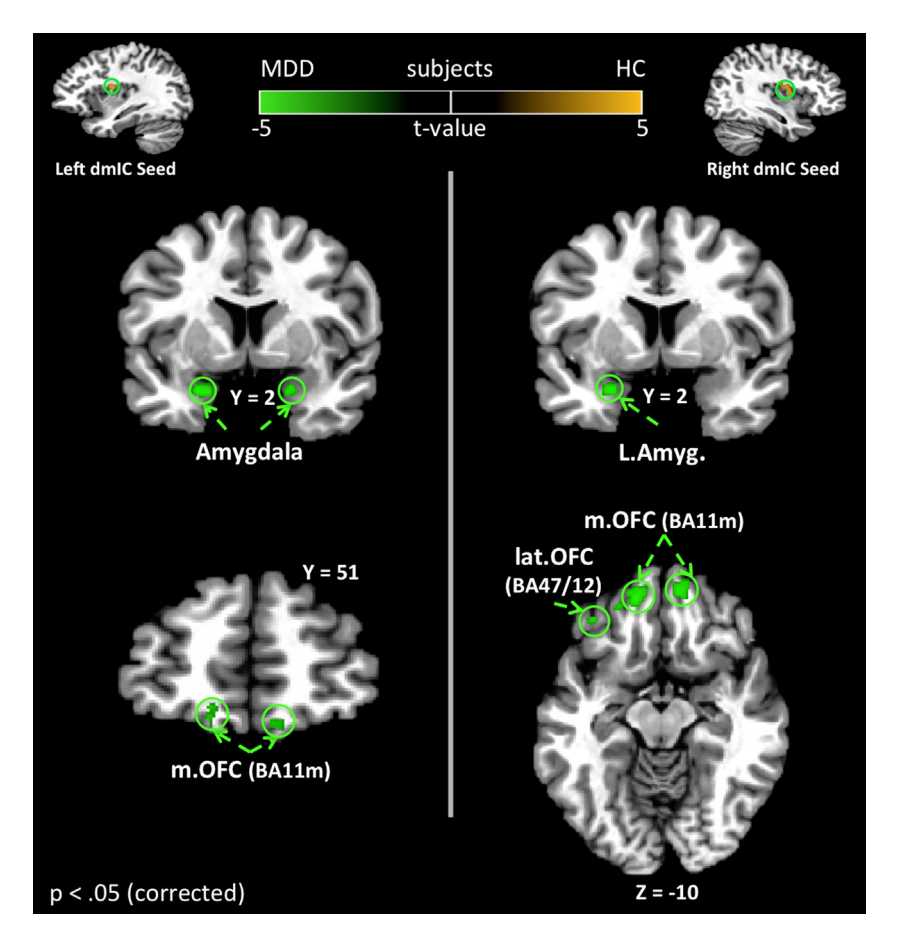


Figure 3. Group differences in blood oxygen level-dependent resting-state functional connectivity to the dorsal mid-insula cortex (dmlC). The left and right dmlC regions, identified in Figure 1, were used as seeds for a comparison of resting-state functional connectivity between healthy (HC) and depressed subjects. Many of the circled regions, including the amygdala (Amyg) and orbitofrontal cortex (OFC), have previously been implicated in the pathophysiology of major depressive disorder (MDD). In the present study, depressed participants exhibited significantly stronger resting-state functional connectivity between these regions and the dmlC. All results corrected for multiple comparisons at *pcorrected* < .05. BA, Brodmann area; L, left; lat, lateral; m, medial.

Table 3. Brain Regions Exhibiting Greater dmIC Resting-State Functional Connectivity in the MDD Subjects Compared with Healthy Participants

| | Peak | Coordin | | Volume | |
|--------------------------|------|---------|-----|-----------------|--------------------|
| Side/Location | х | у | Z | t ₃₈ | (mm ³) |
| Left dmIC Seed | | | | | |
| Depressed > Healthy | | | | | |
| R middle temporal gyrus | +45 | -68 | +7 | -4.66 | 477 |
| L amygdala | -20 | +3 | -19 | -4.04 | 311 |
| R middle occipital gyrus | +27 | -66 | +23 | -4.11 | 268 |
| L medial OFC (BA11m) | -13 | +45 | -10 | -3.37 | 177 |
| R medial OFC (BA11m) | +10 | +52 | -12 | -4.17 | 166 |
| R amygdala | +22 | +3 | -19 | -3.43 | 129 |
| Healthy > Depressed | | | | | |
| R cerebellum | +18 | -75 | -22 | 4.87 | 423 |
| Right dmIC Seed | | | | | |
| Depressed > Healthy | | | | | |
| L medial OFC (BA11m) | -11 | +48 | -8 | -4.55 | 745 |
| R medial OFC (BA11m) | +10 | +53 | -14 | -4.61 | 562 |
| R middle temporal gyrus | +52 | -68 | +13 | -4.29 | 466 |
| R middle occipital gyrus | +25 | -64 | +20 | -3.97 | 316 |
| L precentral gyrus | -29 | -8 | +48 | -4.83 | 263 |
| L amygdala | -24 | +3 | -19 | -3.99 | 198 |
| L lateral OFC (BA47/12) | -36 | +36 | -7 | -3.09 | 118 |

BA, Brodmann area; dmlC, dorsal mid-insula cortex; L, left; MDD, major depressive disorder; OFC, orbitofrontal cortex; R, right.

^aAll coordinates reported according to Talairach stereotaxic atlas (73). This format uses three numbers (x, y, z) to describe the distance from the anterior commissure. The x, y, z dimensions refer to right(+)-to-left(-), anterior(+)-to-posterior(-), and dorsal(+)-to-ventral(-), respectively.

in MDD subjects versus control subjects (Figure 3, Table 3). Functional connectivity between the dmlC and both posterior OFC and sgPFC, regions exhibiting decreased activity during heartbeat attention, was also positively correlated to depression severity. Additionally, dmIC connectivity with both anterior and posterior insula was greater with increasing depression severity.

Comment

Prior findings have demonstrated that MDD is associated with interoceptive deficits assessed behaviorally (4-7) and that the insula contributes to interoception in healthy humans (15-17). These findings warranted the prediction that MDD patients would exhibit abnormal insula hemodynamic activity during interoceptive attention and that this activity would be related to depression severity. Both hypotheses were confirmed in the present study. Within the dorsal mid-insula, as well as a network of brain regions involved in emotion and visceral control, unmedicated and currently depressed adults exhibited decreased activation during interoceptive attention relative to healthy control subjects. This reduced dmIC activity in depression was observed during attention to interoceptive signals broadly (i.e., attention to heartbeat, stomach, and bladder sensations), potentially consistent with evidence that behavioral measures of interoceptive sensitivity are correlated across interoceptive modalities (50). The function of the dorsal mid-insula region identified here has been previously identified as being homeostatically sensitive (24) and selective for interoception (15). Crucially, this region appears to constitute the human homologue of a location identified in macaque monkeys as the terminus of a major vagal afferent pathway, originating from the entrance of the vagus nerve into the solitary nuclear complex in the medulla, through the parvocellular

portion of the ventroposteromedial nucleus of the thalamus, and ending in the dorsal insula/frontal operculum (19-21).

Although relatively more attention has been paid to the role of the anterior insula in mood disorders, there is a growing body of evidence that the dmIC is also critically affected. For example, recent studies have highlighted mood- and anxiety-related abnormalities in dmlC gray matter volume (29), gammaaminobutyric acid-benzodiazepine site binding potential (30), and regional cerebral blood flow (31). Until the present study, however, the functional significance of these findings had not been explored. Our data suggest that structural and functional abnormalities in the dmIC present in depressed subjects may lead to altered information processing of interoceptive signals, as indexed by the diminished hemodynamic response of the insula during interoceptive attention.

Hemodynamic response during heartbeat interoception was significantly negatively correlated with HDRS symptom severity in the dmIC, as was the relationship between hemodynamic response and severity of somatic symptoms. Additionally, a relationship between depression severity and BOLD activity during interoception was observed in the amygdala, as well as in the ventral anterior insula and ventral mid-insula. The ventral anterior region of the insula implicated here is rostrally contiguous with the caudal orbitofrontal cortex and is the insula region most strongly associated with emotion (22,49). Additionally, ventral anterior insula metabolism may also serve as a predictive measure of response to distinct treatment methods for depression (32).

Recently, Paulus and Stein (13) have theorized that amplification of interoceptive signals within the insula contributes to the pathogenesis of depression. By this account, the emotional dysregulation and negative affect associated with MDD (2) result from amplified interoceptive background noise that interferes with an individual's ability to generate accurate predictions about how external stimuli will affect one's homeostatic state and general well-being. We envision at least two scenarios by which increased basal noise within the dmlC might contribute to the pathology of MDD. First, the finding in the present study that resting-state functional connectivity between the amygdala and the dmIC is not only increased in MDD but is also predictive of depression severity suggests that interoceptive deficits and amygdala pathophysiology in MDD may be functionally related. Pathologically increased amygdala activity in MDD subjects (33,51) might propagate to the insula, thereby leading to maladaptive information processing in this region. The resulting reduced interoceptive signal-to-noise ratio could thus interfere with depressed subjects' ability to reliably discriminate afferent homeostatic signals, perhaps also causing a form of emotional allodynia (52,53) (i.e., where psychic pain or visceral discomfort is caused by a nonpainful stimulus), conceivably accounting for the idiopathic pain states that commonly manifest in MDD (1). This is supported by recent evidence implicating the dmIC in the interaction between chronic pain and depression (52,54,55), as well as the present study's finding of increased dmIC connectivity in depressed subjects to anterior and posterior insula regions associated with emotional and pain processing (56-58). Alternately, peripheral pathology, perhaps due to heightened pain responses (1) or chronic inflammation (59,60), which directly affects dmIC function (61), could be propagated to the amygdala, heightening its activity and resulting in the exaggerated emotional responses and negative emotional processing bias observed in MDD (33,51,62). The precise origin of this increased basal noise in the dmIC, whether peripheral or limbic, cannot be inferred from the present data, due to the multiple reciprocal neural connections along the entire length of the insula (36,37) (see Supplemental Discussion in Supplement 1 for more discussion on interoception in anxiety and depression). Ultimately, due to the difficulties inherent in interpreting group differences in hemodynamic response, our data cannot elucidate the specific pathophysiology underlying the abnormal BOLD activity observed during interoception in MDD. Future studies using other imaging modalities that can provide more direct assays of neural activity (e.g., electrophysiological or glucose metabolic activity) within the dmIC during interoception may be helpful in resolving this question.

Consistent with previous findings in resting-state studies of MDD, depressed subjects exhibited increased functional connectivity between default mode network regions, such as the sgPFC (35,42,63), as well as brain regions previously implicated in the pathophysiology of depression, most notably the amygdala and OFC (33,38). Major depressive disorder is associated with neuropathological and neuroimaging abnormalities within the sgPFC (33,40,41) and cerebral blood flow and glucose metabolism in the sgPFC also correlate with depression severity (33,64). Based upon cytoarchitecture and connectivity, Öngür et al. (49) suggest that BA32pl is the human homologue of rodent prelimbic cortex, a region associated with the enhancement of fear responses mediated via the amygdala (49,65) [this region is adjacent to but distinct from BA25, a region of sgPFC considered to be the human homologue of infralimbic cortex (49), which also has been implicated in depression (66,67)]. Given our observation that both the amygdala and the sgPFC (BA32pl) exhibited functional connectivity to the dmIC that was positively correlated with depression severity, the present study offers neurophysiological findings that appear compatible with preclinical evidence that activity within this region increases emotional expression mediated via the central nucleus of the amygdala (65).

Similarly, volumetric abnormalities as well as increased regional cerebral blood flow and metabolism in the OFC have been reported in neuroimaging and postmortem neuropathological studies of MDD (33,39,68), and lesions of the OFC increase the risk for developing MDD (69). The posterior OFC (BA13a) constitutes one of the three areas identified by Öngür and Price (70) as forming critical junctions between the medial (visceromotor) and orbital (sensory) prefrontal cortical networks (38,49). The other two junction areas between these networks, BA45a and BA12o/47s, previously were shown to exhibit increased cerebral blood flow and metabolism in MDD (38,71). The involvement of BA13a in decreased interoceptive activity observed in depressed subjects in the present study, as well as the significant correlation between functional connectivity to the dmlC and depression severity, implicate this region in the pathophysiology of MDD as well. The involvement of this area of convergence between networks is noteworthy because the other PFC areas where abnormalities were observed in depressed patients under interoception and under resting connectivity with dmlC implicate both the medial prefrontal (sgPFC) and the orbital (OFC regions 111 and 11m) networks (Tables 2 and 3; Figures 2 and 3) (38,49,70).

Conclusion

Major depressive disorder is associated with a reduced hemodynamic response during interoception within the dmIC, a primary viscerosensory region of the insula, as well as in a network of regions involved in emotional and visceral control, many of which have been implicated previously in depression.

Additionally, ventral anterior and ventral and dorsal mid-insula hemodynamic activity during interoception correlates inversely with depression severity. This reduction in task-related activity is accompanied by greater functional connectivity between the dmIC and this network of regions under the resting condition to an extent that is positively correlated with depression severity. Consistent with the findings of this study, the vagal nerve stimulation-induced BOLD response, specifically within right dmIC, is positively correlated with HDRS scores in treatmentresistant depression (72). Combined with its role in vagal afferent signaling and extensive limbic connectivity, these findings suggest that changes in dmIC activity play a mechanistic role in the efficacy of vagal nerve stimulation treatment for depression. Future studies are needed to determine if the abnormal interoceptive activity we observed reflects a state or trait effect by assessing the hemodynamic correlates of interoception in individuals studied in the remitted condition of MDD and individuals who are at high familial risk for developing MDD. It will also be important to explore the effect of antidepressant medications on group differences in interoception and the mechanisms by which pharmacologic interventions may exert their influence in this region of the cortex. The findings of the present study demonstrate that abnormal activity and connectivity within primary viscerosensory regions of the insula play an important role in the depressive symptoms experienced by individuals with MDD and may offer a promising therapeutic target for depression.

This research was supported by the National Institute of Mental Health (K01MH096175-01) grant to WKS, a grant from the Oklahoma Center for the Advancement of Science and Technology (OCAST HR10-141) to WKS, a National Alliance for Research on Schizophrenia and Depression Young Investigator Award to WKS, and a grant to WKS from the Oklahoma Tobacco Research Center, the Laureate Institute for Brain Research, and The William K. Warren Foundation. JAA was also supported by the Wilfred A. Woobank Fellowship from the University of Tulsa.

We thank Kara Kerr for assistance with data management and Rayus Kuplicki for assistance with resting-state data preprocessing, as well as Joan Collins, Jessica Santiago, Lisa Kinyon, and Michele Drevets for their help with subject assessment and recruitment.

WCD has consulted for Johnson & Johnson Pharmaceuticals, Inc. and RBM/Myriad, Inc. and currently is an employee of Johnson & Johnson, Inc. All other authors report no biomedical financial interests or potential conflicts of interest.

Supplementary material cited in this article is available online at http://dx.doi.org/10.1016/j.biopsych.2013.11.027.

- 1. Lépine J-P, Briley M (2004): The epidemiology of pain in depression. *Hum Psychopharmacol* 19(suppl 1):S3–S7.
- Henningsen P, Zimmermann T, Sattel H (2003): Medically unexplained physical symptoms, anxiety, and depression: A meta-analytic review. Psychosom Med 65:528–533.
- 3. Willem Van der Does AJ, Antony MM, Ehlers A, Barsky AJ (2000): Heartbeat perception in panic disorder: A reanalysis. *Behav Res Ther* 38:47–62.
- Mussgay L, Klinkenberg N, Rüddel H (1999): Heart beat perception in patients with depressive, somatoform, and personality disorders. J Psychophysiol 13:27–36.
- Dunn BD, Dalgleish T, Ogilvie AD, Lawrence AD (2007): Heartbeat perception in depression. Behav Res Ther 45:1921–1930.
- Pollatos O, Traut-Mattausch E, Schandry R (2009): Differential effects of anxiety and depression on interoceptive accuracy. *Depress Anxiety* 26: 167–173.

- 7. Terhaar J, Viola FC, Bär K-J, Debener S (2012): Heartbeat evoked potentials mirror altered body perception in depressed patients. Clin Neurophysiol 123:1950-1957.
- 8. Furman DJ, Waugh CE, Bhattacharjee K, Thompson RJ, Gotlib IH (2013): Interoceptive awareness, positive affect, and decision making in major depressive disorder. J Affect Disord 151:780-785.
- 9. Damasio AR (1996): The somatic marker hypothesis and the possible functions of the prefrontal cortex. Philos Trans R Soc Lond B Biol Sci 351:1413-1420.
- 10. Pollatos O, Gramann K, Schandry R (2007): Neural systems connecting interoceptive awareness and feelings. Hum Brain Mapp 28:9-18.
- 11. Herbert BM, Pollatos O, Schandry R (2007): Interoceptive sensitivity and emotion processing: An EEG study. Int J Psychophysiol 65:214-227.
- 12. Honkalampi K, Hintikka J, Laukkanen E, Lehtonen J, Viinamäki H (2001): Alexithymia and depression: A prospective study of patients with major depressive disorder. Psychosomatics 42:229-234.
- 13. Paulus MP, Stein MB (2010): Interoception in anxiety and depression. Brain Struct Funct 214:451-463.
- 14. Domschke K, Stevens S, Pfleiderer B, Gerlach AL (2010): Interoceptive sensitivity in anxiety and anxiety disorders: An overview and integration of neurobiological findings. Clin Psychol Rev 30:1-11.
- 15. Simmons WK, Avery JA, Barcalow JC, Bodurka J, Drevets WC, Bellgowan P (2013): Keeping the body in mind: Insula functional organization and functional connectivity integrate interoceptive, exteroceptive, and emotional awareness. Hum Brain Mapp 34: 2944-2958
- 16. Critchley HD, Wiens S, Rotshtein P, Ohman A, Dolan RJ (2004): Neural systems supporting interoceptive awareness. Nat Neurosci 7:189-195.
- 17. Khalsa SS, Rudrauf D, Feinstein JS, Tranel D (2009): The pathways of interoceptive awareness. Nat Neurosci 12:1494-1496.
- 18. Craig AD (2002): How do you feel? Interoception: The sense of the physiological condition of the body. Nat Rev Neurosci 3:655-666.
- 19. Beckstead RM, Morse JR, Norgren R (1980): The nucleus of the solitary tract in the monkey: Projections to the thalamus and brain stem nuclei. J Comp Neurol 190:259-282.
- 20. Pritchard TC, Hamilton RB, Morse JR, Norgren R (1986): Projections of thalamic gustatory and lingual areas in the monkey, Macaca fascicularis. J Comp Neurol 244:213-228.
- 21. Carmichael ST, Price JL (1995): Sensory and premotor connections of the orbital and medial prefrontal cortex of macaque monkeys. J Comp Neurol 363:642-664.
- 22. Kurth F, Zilles K, Fox PT, Laird AR, Eickhoff SB (2010): A link between the systems: Functional differentiation and integration within the human insula revealed by meta-analysis. Brain Struct Funct 214:
- 23. Kelly C, Toro R, Di Martino A, Cox CL, Bellec P, Castellanos FX, Milham MP (2012): A convergent functional architecture of the insula emerges across imaging modalities. Neuroimage 61:1129-1142.
- 24. Simmons WK, Rapuano KM, Kallman SJ, Ingeholm JE, Miller B, Gotts SJ, et al. (2013): Category-specific integration of homeostatic signals in caudal but not rostral human insula. Nat Neurosci 16:1551-1552.
- 25. Pollatos O, Schandry R, Auer DP, Kaufmann C (2007): Brain structures mediating cardiovascular arousal and interoceptive awareness. Brain Res 1141:178-187.
- 26. Farb NAS, Segal ZV, Anderson AK (2013): Attentional modulation of primary interoceptive and exteroceptive cortices. Cereb Cortex 23: 114-126.
- 27. Wang G-J, Tomasi D, Backus W, Wang R, Telang F, Geliebter A, et al. (2008): Gastric distention activates satiety circuitry in the human brain. Neuroimage 39:1824-1831.
- 28. Stephan E, Pardo JV, Faris PL, Hartman BK, Kim SW, Ivanov EH, et al. (2003): Functional neuroimaging of gastric distention. J Gastrointest
- 29. Sprengelmeyer R, Steele JD, Mwangi B, Kumar P, Christmas D, Milders M, Matthews K (2011): The insular cortex and the neuroanatomy of major depression. J Affect Disord 133:120-127
- 30. Cameron OG, Huang GC, Nichols T, Koeppe RA, Minoshima S, Rose D, Frey KA (2007): Reduced gamma-aminobutyric acid(A)-benzodiazepine binding sites in insular cortex of individuals with panic disorder. Arch Gen Psychiatry 64:793–800.
- 31. Jabbi M, Kippenhan JS, Kohn P, Marenco S, Mervis CB, Morris CA, et al. (2012): The Williams syndrome chromosome 7g11.23 hemideletion

- confers hypersocial, anxious personality coupled with altered insula structure and function. Proc Natl Acad Sci U S A 109:E860-E866.
- 32. McGrath CL, Kelley ME, Holtzheimer PE, Dunlop BW, Craighead WE, Franco AR, et al. (2013): Toward a neuroimaging treatment selection biomarker for major depressive disorder. JAMA Psychiatry 70: 821-829.
- 33. Drevets WC, Price JL, Furey ML (2008): Brain structural and functional abnormalities in mood disorders: Implications for neurocircuitry models of depression. Brain Struct Funct 213:93-118.
- 34. Phillips ML, Drevets WC, Rauch SL, Lane R (2003): Neurobiology of emotion perception I: The neural basis of normal emotion perception. Biol Psychiatry 54:504-514.
- 35. Greicius MD, Flores BH, Menon V, Glover GH, Solvason HB, Kenna H, et al. (2007): Resting-state functional connectivity in major depression: Abnormally increased contributions from subgenual cingulate cortex and thalamus. Biol Psychiatry 62:429-437.
- 36. Augustine JR (2003): Circuitry and functional aspects of the insular lobe in primates including humans. Brain Res Brain Res Rev 22: 229-244.
- 37. Mesulam MM, Mufson EJ (1982): Insula of the old world monkey. III: Efferent cortical output and comments on function. J Comp Neurol 212:38-52.
- 38. Price JL, Drevets WC (2010): Neurocircuitry of mood disorders. Neuropsychopharmacology 35:192-216.
- 39. Lorenzetti V, Allen NB, Fornito A, Yücel M (2009): Structural brain abnormalities in major depressive disorder: A selective review of recent MRI studies. J Affect Disord 117:1-17.
- 40. Drevets WC, Price JL, Simpson JR, Todd RD, Reich T, Vannier M, Raichle ME (1997): Subgenual prefrontal cortex abnormalities in mood disorders. Nature 386:824-827.
- 41. Ongür D, Drevets WC, Price JL (1998): Glial reduction in the subgenual prefrontal cortex in mood disorders. Proc Natl Acad Sci U S A 95: 13290-13295
- 42. Kühn S, Gallinat J (2013): Resting-state brain activity in schizophrenia and major depression: A quantitative meta-analysis. Schizophr Bull 39: 358-365.
- 43. Hamilton M (1960): A rating scale for depression. J Neurol Neurosurg Psychiatry 23:56-62.
- 44. Hamilton M (1959): The assessment of anxiety states by rating. Br J Med Psychol 32:50-55
- 45. Jäncke L, Mirzazade S, Shah NJ (1999): Attention modulates activity in the primary and the secondary auditory cortex: A functional magnetic resonance imaging study in human subjects. Neurosci Lett 266: 125-128.
- 46. Johansen-Berg H, Christensen V, Woolrich M, Matthews PM (2000): Attention to touch modulates activity in both primary and secondary somatosensory areas. Neuroreport 11:1237-1241.
- 47. Somers DC, Dale AM, Seiffert AE, Tootell RB (1999): Functional MRI reveals spatially specific attentional modulation in human primary visual cortex. Proc Natl Acad Sci U S A 96:1663-1668.
- 48. Cleary P, Guy W (1977): Factor analysis of the Hamilton depression scale. Drugs Exp Clin Res 1:115-120.
- 49. Ongür D, Ferry AT, Price JL (2003): Architectonic subdivision of the human orbital and medial prefrontal cortex. J Comp Neurol 460:425-449.
- 50. Herbert BM, Muth ER, Pollatos O, Herbert C (2012): Interoception across modalities: On the relationship between cardiac awareness and the sensitivity for gastric functions. PLoS One 7:e36646.
- 51. Drevets WC (2003): Neuroimaging abnormalities in the amygdala in mood disorders. Ann N Y Acad Sci 985:420-444.
- 52. Mutschler I, Ball T, Wankerl J, Strigo IA (2012): Pain and emotion in the insular cortex: Evidence for functional reorganization in major depression. Neurosci Lett 520:204-209.
- 53. Strigo IA, Simmons AN, Matthews SC, Craig AD, Paulus MP (2008): Increased affective bias revealed using experimental graded heat stimuli in young depressed adults: Evidence of "emotional allodynia". Psychosom Med 70:338-344.
- 54. Giesecke T, Gracely RH, Williams DA, Geisser ME, Petzke FW, Clauw DJ (2005): The relationship between depression, clinical pain, and experimental pain in a chronic pain cohort. Arthritis Rheum 52:1577-1584.
- 55. Seifert CL, Valet M, Pfaffenrath V, Boecker H, Rüther KV, Tölle TR, Sprenger T (2011): Neurometabolic correlates of depression and disability in episodic cluster headache. J Neurol 258:123-131.

- Singer T, Seymour B, O'Doherty J, Kaube H, Dolan RJ, Frith CD (2004): Empathy for pain involves the affective but not sensory components of pain. Science 303:1157–1162.
- 57. Craig AD, Chen K, Bandy D, Reiman EM (2000): Thermosensory activation of insular cortex. *Nat Neurosci* 3:184–190.
- 58. Henderson LA, Gandevia SC, Macefield VG (2007): Somatotopic organization of the processing of muscle and cutaneous pain in the left and right insula cortex: A single-trial fMRI study. *Pain* 128:20–30.
- Miller AH, Maletic V, Raison CL (2009): Inflammation and its discontents: The role of cytokines in the pathophysiology of major depression. *Biol Psychiatry* 65:732–741.
- **60.** Thayer JF, Sternberg EM (2010): Neural aspects of immunomodulation: Focus on the vagus nerve. *Brain Behav Immun* 24:1223–1228.
- 61. Harrison NA, Brydon L, Walker C, Gray MA, Steptoe A, Dolan RJ, Critchley HD (2009): Neural origins of human sickness in interoceptive responses to inflammation. *Biol Psychiatry* 66:415–422.
- **62.** Elliott R, Rubinsztein JS, Sahakian BJ, Dolan RJ (2002): The neural basis of mood-congruent processing biases in depression. *Arch Gen Psychiatry* 59:597–604.
- **63.** Li B, Liu L, Friston KJ, Shen H, Wang L, Zeng L-L, Hu D (2013): A treatment-resistant default mode subnetwork in major depression. *Biol Psychiatry* 74:48–54.
- **64.** Drevets WC (2000): Functional anatomical abnormalities in limbic and prefrontal cortical structures in major depression. *Prog Brain Res* 126:413–431.

- Burgos-Robles A, Vidal-Gonzalez I, Quirk GJ (2009): Sustained conditioned responses in prelimbic prefrontal neurons are correlated with fear expression and extinction failure. J Neurosci 29:8474–8482.
- **66.** Mayberg HS, Lozano AM, Voon V, McNeely HE, Seminowicz D, Hamani C, *et al.* (2005): Deep brain stimulation for treatment-resistant depression. *Neuron* 45:651–660.
- 67. Drevets WC, Savitz J, Trimble M (2008): The subgenual anterior cingulate cortex in mood disorders. CNS Spectr 13:663–681.
- **68.** Drevets WC (2000): Neuroimaging studies of mood disorders. *Biol Psychiatry* 48:813–829.
- MacFall JR, Payne ME, Provenzale JE, Krishnan KR (2001): Medial orbital frontal lesions in late-onset depression. *Biol Psychiatry* 49: 803–806.
- Ongür D, Price JL (2000): The organization of networks within the orbital and medial prefrontal cortex of rats, monkeys and humans. Cereb Cortex 10:206–219.
- 71. Drevets WC, Videen TO, Price JL, Preskorn SH, Carmichael ST, Raichle ME (1992): A functional anatomical study of unipolar depression. *J Neurosci* 12:3628–3641.
- 72. Nahas Z, Teneback C, Chae J-H, Mu Q, Molnar C, Kozel FA, et al. (2007): Serial vagus nerve stimulation functional MRI in treatment-resistant depression. Neuropsychopharmacology 32:1649–1660.
- 73. Talairach J, Tournoux JTP (1988): Co-planar Stereotaxic Atlas of the Human Brain. New York: Thieme Medical Publishers.

Major Depressive Disorder Is Associated with Abnormal Interoceptive Activity and Functional Connectivity in the Insula

Supplemental Information

Table of Contents

- 1. Supplemental Methods
 - a. Additional imaging task details
 - b. Heart rate analysis
 - c. Imaging scan parameters
 - d. Data preprocessing
 - e. Subject-level statistical analyses
 - f. Resting scan preprocessing
 - g. Motion censoring/additional motion correction
 - h. Resting-state functional connectivity analyses
 - i. Correction for multiple comparisons and anatomical ROI definitions
- 2. Supplemental Results
 - a. Demographic and clinical characteristics
 - b. Focused Awareness task ratings
 - c. Comorbidity within MDD subjects
 - d. The hemodynamic response to interoception and other behavioral measures
 - e. Functional connectivity of the dmIC and other behavioral measures
 - f. Additional group differences in stomach and bladder interoception
- 3. Supplemental Discussion
 - a. Depression, anxiety, and interoceptive awareness
 - b. The Focused Awareness task
- 4. Supplemental Tables
 - a. Table S1. Focused Awareness task ratings
 - b. Table S2. Group differences in dmlC activity during stomach and bladder interoception
 - c. Table S3. Correlation of dmIC activity during interoception with total HDRS and HARS rating scale scores in the depressed subjects
 - d. Table S4. Correlation of dmIC activity during heartbeat interoception with HDRS subscales in depressed subjects from (Cleary and Guy, (10))
 - e. Table S5. Brain regions where the hemodynamic response to heartbeat interoception was correlated with depression severity
 - f. Table S6. Brain regions where functional connectivity with the dmlC was correlated with depression severity
 - g. Table S7. Comparison of MDD subjects with and without secondary comorbid anxiety disorders
 - h. Table S8. Comparison of dmlC activity during heartbeat interoception between MDD subjects with and without comorbid anxiety disorders
 - i. Table S9. Correlation of dmIC activity during interoception with MDE duration in the depressed subjects
 - j. Table S10. Brain regions where the hemodynamic response to heartbeat interoception was correlated with somatic symptom severity
 - k. Table S11. Brain regions where functional connectivity with the dmIC was correlated with somatic symptom severity
 - I. Table S12. Brain regions exhibiting differences in the hemodynamic response to stomach and bladder interoception between healthy and depressed subjects

5. Supplemental Figures

- a. Figure S1. Group differences in stomach and bladder interoception
- b. Figure S2. Brain regions where activation during heartbeat interoception is correlated with depression severity
- c. Figure S3. Dorsal mid-insula resting-state functional connectivity is correlated with depression severity
- d. Figure S4. TSNR maps
- e. Figure S5. Group differences in stomach and bladder interoception
- 6. Supplemental References

Supplemental Methods

Additional Imaging Task Details

After the resting scan, but prior to the start of the Focused Awareness scans, we presented to each subject a three-minute practice version of the task while they lay in the scanner. This shortened practice version of the task included all interoceptive and exteroceptive conditions present within the full task, as well as rating periods for all task conditions. We observed participants throughout these practice sessions and ensured both that they were able to use the scroll-wheel to make responses and that they fully understood the requirements of the task itself.

In each of the three functional magnetic resonance imaging (fMRI) task scanning runs, we presented the task conditions in a pseudo-random order optimized for fMRI analysis by Optseq2 (http://surfer.nmr.mgh.harvard.edu/optseq/). Each condition trial was separated by a variable-duration interstimulus interval lasting between 2.5 and 22.5-seconds (mean interval = 6.7 seconds), during which time subjects saw only a black fixation mark against a white background. Stimuli were projected onto a screen located inside the scanner bore and viewed through a mirror system mounted on the head-coil. We controlled stimulus presentation and response collection using Eprime2 software (www.pstnet.com). Upon entering the scanner, subjects first underwent a 7 minute 30 second resting-state fMRI scan, during which they viewed a black fixation-cross presented against a white background. We instructed subjects to focus on the fixation-cross, and that for the duration of the resting scan they were simply to clear their mind and not think of anything in particular.

Heart Rate Analysis

We analyzed the pulse oximetry recordings for the resting and Focused Awareness task scans using the suite of 1D analysis tools available within the AFNI software package as follows. For each 10-second period during the scans (45 during the resting scan, and 55 during each Focused Awareness task scan), we normalized the pulse oximetry recording to a maximum intensity of 1 within the 10-second window and raised the intensity values to the 4th power, in order to account for low-level noise

within the recorded signal. We then calculated the derivative of the signal to isolate local signal peaks and multiplied the output by a step function to isolate time points with a positive slope. The result was a binary output with a '1' representing each individual heartbeat within the 10-second window. We subsequently calculated the average R-R distance (the time between individual heart beats) within each 10-second period and averaged the resulting values to obtain the mean R-R distance for each scan. We then divided the number corresponding to the pulse oximeter sampling frequency (50 hz x 60 seconds = 3000) by the average R-R distance to obtain the average heart rate throughout the scan. The output of this procedure on each 10-second scan window was visually confirmed alongside the raw pulse oximeter recording to ensure accurate labeling of each heartbeat within that 10-second window.

We obtained the resting heart rate for each subject by applying this procedure to the pulse oximeter recording from each subject's resting scan. Likewise, we applied this procedure to the output from each Focused Awareness task scan and took the average of the three scans to obtain overall heart rate during the task. To calculate average heart rate during heartbeat interoception trials, we ran this procedure only on the 10-second time period corresponding to each heartbeat interoception trial during the Focused Awareness task scans and then calculated the average heart rate during those periods.

Imaging Scan Parameters

We used the following echo-planar imaging (EPI) imaging parameters for the three task scanning runs: field of view (FOV)/slice/gap = 240/2.9/0 mm, axial slices per volume = 46, acquisition matrix = 96×96 , repetition/echo time TR/TE = 2500/30 ms, SENSE acceleration factor R = 2 in the phase encoding (anterior-posterior) direction, flip angle = 90° , sampling bandwidth = 250 kHz, number of volumes = 220, scan time = 550 sec. We used the same EPI imaging parameters for the resting-state scan, except for: TE = 25 ms, number of volumes = 180, scan time = 450 sec. All EPI images were reconstructed into a 128×128 matrix, in which the resulting fMRI voxel volume was $1.875 \times 1.875 \times 2.9$ mm³. As demonstrated by measurements of temporal signal-tonoise ratio (TSNR), these scan parameters ensured high image quality and reduced

magnetic susceptibility artifacts within limbic regions, including the orbitofrontal cortex (OFC) and subgenual prefrontal cortex (sgPFC) (see Figure S4). We used a T1-weighted magnetization-prepared rapid gradient-echo sequence with SENSE to provide an anatomical reference for the fMRI analysis. The anatomical scan had the following parameters: FOV = 240 mm, axial slices per volume = 176, slice thickness = 0.9 mm, image matrix = 256 x 256, voxel volume 0.938 x 0.938 x 0.9 mm 3 , TR/TE = 5/2.02 ms, acceleration factor R = 2, flip angle = 8° , inversion time TI = 725 ms, sampling bandwidth = 31.25 kHz, scan time = 372 sec.

Data Preprocessing

We registered the anatomical scan to the first volume of the resting-state EPI time-course using AFNI's anatomical-to-epi alignment procedure. We then spatially transformed the anatomical scan to the stereotaxic array of Talairach and Tournoux (1) using AFNI's automated algorithm and the transformation parameters were saved for use later in the preprocessing. We excluded the first 4 volumes of each EPI time-course from data analysis to allow the fMRI signal to reach steady state. Subsequently, we applied a slice timing correction to all EPI volumes. We saved estimates of the transformations necessary to register all EPI volumes to the first volume of the first EPI time-course both for the next step in the preprocessing and also for use in the statistical analyses. We implemented motion correction and spatial transformation of the EPI data in a single image transformation, and resampled all images to a 1.75 x 1.75 x 1.75 mm³ grid. We then smoothed the EPI data with a 6-mm full-width at half-maximum (FWHM) Gaussian kernel, and normalized the signal intensity for each EPI volume to reflect percent signal change from each voxel's mean intensity across the time-course.

Subject-level Statistical Analyses

The regression model included regressors for each interoceptive attention condition and the exteroception condition. To adjust the model for the shape and delay of the blood oxygenation level-dependent (BOLD) function, we constructed the task regressors by convolution of a gamma-variate function and a boxcar function having a 10-second width (or 5-second width for modeling response periods) beginning at the

onset of each occurrence of the condition. Additionally, the regression model included regressors of non-interest to account for each run's signal mean, linear, quadratic, and cubic signal trends, as well as the 6 normalized motion parameters (3 translations, 3 rotations) computed during the image registration preprocessing.

Resting Scan Preprocessing

For preprocessing of the resting-state scans, we employed a modified version of the ANATICOR method (2), implemented through the AFNI program afni restproc.py (available in the AFNI binaries distributed through the AFNI website). We excluded the first 4 volumes of the resting state-scan in order to remove T1 effects in the data. We then used a de-spiking interpolation algorithm (AFNI's 3dDespike) to remove any transient signal spikes from the data that might artificially inflate estimates of the correlation among voxels' time-series, followed by slice time correction. We then registered each volume in the resting state EPI time-course to the first volume (which was registered to the anatomical scan). We constructed masks of the subject's ventricles and white matter from the subject's anatomical scan using FreeSurfer (http://surfer.nmr.mgh.harvard.edu/), and eroded each mask slightly to prevent partial volume effects that might include signal from gray matter voxels in the mask. First we calculated the average time course during the resting-state run within the ventricle mask. Next, to produce estimates of the local physiological noise, we calculated for each gray matter voxel the average signal time-course for all white matter voxels within a 1.5 cm radius. We also used the respiration and cardiac traces collected during the resting-state scan to calculate RETROICOR (3) and respiration volume per time (RVT) (4) parameters using the RetroTS.m plugin for MATLAB. We then removed the mean, linear, quadratic, and cubic trends from all the regressors of non-interest described above. In total, the estimates of physiological and non-physiological noise included the 6 motion parameters (3 translations, 3 rotations), the average ventricle signal, the average local white matter signal, and 13 respiration regressors from RETROICOR and RVT. We constructed the predicted time-course for these nuisance variables using AFNI's 3dTfitter program, and then subtracted this predicted time-course from each resting-state voxel time-course, yielding a residual time-course for each voxel. We then

smoothed this residual resting-state time-course with a 6 mm FWHM Gaussian kernel, resampled it to a 1.75 mm x 1.75 mm x 1.75 mm grid, and spatially transformed it to stereotaxic space for all subsequent analyses.

Motion Censoring/Additional Motion Correction

Recently, much attention has been paid to the possibility that uncontrolled subject motion can induce artifactual group differences in resting-state functional connectivity analyses (5; 6). We thus implemented motion-censoring algorithms (a.k.a. "scrubbing") to guard against this possibility in the present study. In order to remove any additional motion related signal artifacts that were still present after regression of motion parameters, we implemented a censoring technique to identify and remove any time point with motion above a certain predefined threshold. We used the AFNI program 1d_tool.py on the 6 motion parameters created during the volume registration step. The output was a single time series reflecting the Euclidean normalized derivative of the motion parameters. We then thresholded this time series, so that any time point where the derivative was greater than 0.3 (roughly 0.3 mm motion) was censored. We also used the AFNI program 3dToutcount to plot the fraction of voxels within a brain mask per time point that were considered outliers. The source of these outliers could include head motion or miscellaneous signal artifacts. We then censored any time point where greater than 5% of brain voxels were considered outliers. We then combined these lists of censored time points created by both methods to create a list of time points censored by both methods. We provided this combined list to the AFNI program 3dDeconvolve, which removed those time points from consideration during the subsequent regression analysis.

Resting-State Functional Connectivity Analyses

At the subject-level, we constructed the seed time-series for both of the dorsal mid-insula regions of interest (ROIs) identified in the heartbeat interoception contrast (Figure 1) by calculating the average time series during the resting-state scan within the ROIs. Using multiple regression analysis, we produced maps of the time-course correlations (r-values) between both of the seed regions and all other voxels in the

brain. We then transformed these r-values to Z-scores. To identify voxels exhibiting group differences in spontaneous BOLD fluctuations correlated with the insular seed regions, we implemented group-level random effects t-tests comparing the Z-scores generated for the healthy subjects against the Z-scores generated for the depressed subjects. We corrected all resulting statistical maps for multiple comparisons at p < .05 (using the method described below).

To identify regions where resting-state functional connectivity to the insula was associated with depression severity, we examined the correlation between functional connectivity Z-scores for both insula seed regions and the total Hamilton Depression Rating Scale (HDRS) scores of the depressed subjects. We performed a one-sample t-test, using the depressed subjects' HDRS scores entered as a covariate, in order to determine if the correlation coefficient for the relationship between Z-scores and HDRS scores within each voxel was significantly different from 0. Resultant maps were cluster-size corrected for multiple comparisons at p < .05 as mentioned below.

Correction for Multiple Comparisons and Anatomical ROI Definitions

All voxel-wise statistical maps created for analysis of task data and resting-state data were corrected for multiple comparisons at p < .05 as follows. Within a prioridefined regions of interest, we used a voxel-wise p-value of .01 and a small-volume correction for multiple comparisons using Monte Carlo simulations of cluster size. Those regions included the insular cortex, the amygdala, the orbitofrontal cortex, the caudate, and the ventromedial prefrontal cortex. Outside of these regions of interest we used a voxel-wise threshold of p < .001, combined with Monte Carlo simulations of cluster size. We subsequently applied a mask to all contrast maps (see Figure S4) to ensure that in all brain regions exhibiting group differences in interoception or functional connectivity, the TSNR was greater than 40 (Figure S4), allowing for reliable detection of effects between conditions (7).

The regions-of-interest defined *a priori* in the amygdala and caudate were defined using pre-rendered stereotaxic ROI masks available in AFNI. These ROI masks are part of an anatomical atlas based on probability maps generated for 35 cortical areas (8) and the parcellation of cortical and subcortical structures (of the AFNI

Talairach N27 atlas brain) generated by the FreeSurfer program. The left and right insula region-of-interest masks were also generated by the FreeSurfer program, which we applied to the AFNI Talairach N27 atlas brain.

The anterior OFC ROI was bounded posteriorly by a line drawn at the anterior edge of the genu of the corpus callosum (Y = 32 on the AFNI Talairach N27 atlas brain). The ROI was bounded anteriorly by the frontal pole (Y = 61), and ventrally by the ventral edge of the cortex (at approximately Z = -19). Dorsally, the OFC ROI extended up to the fundus of the transverse orbital sulcus, and medially to the medial edge of the medial orbital gyrus (according to the methods defined by Chiavaras *et al.*, 2001 (9)). Laterally, the ROI extended to the edge of the lateral intermediate orbital sulcus or the lateral orbital sulcus, whichever of the two was located more medially.

The ventromedial prefrontal cortex (vmPFC) ROI was bounded anteriorly by a line drawn at the anterior edge of the genu of the corpus callosum (Y = 31 on the AFNI Talairach N27 atlas brain; which ensured that the OFC and vmPFC ROIs did not overlap) and posteriorly by a line drawn at the posterior edge of the genu (Y = 9). The ROI was bounded medially and ventrally by the medial and ventral surfaces of the cortex, respectively. Dorsally, the ROI extended to the fundus of the olfactory sulcus and the corpus callosum. Laterally, the vmPFC ROI extended to the lateral edge of the olfactory sulcus.

Supplemental Results

Demographic and Clinical Characteristics

The demographic and clinical characteristics of the study samples are listed in Table 1. As expected, the healthy and depressed groups differed significantly on measures of depression (HDRS: $t_{38} = -12.0$, p < .001) and anxiety (Hamilton Anxiety Rating Scale (HARS): $t_{38} = -13.6$, p < .001). The mean age did not differ significantly between groups ($t_{38} = -1.3$, p = .20), nor did body mass index ($t_{38} = -.3$, p = .79).

Resting heart rate, obtained during the resting scan, did not differ between depressed and healthy subjects ($t_{38} = .5$, p = .63; Table 1). Average heart rate during

the Focused Awareness task also did not differ between subjects (t_{38} = .8, p = .43). Additionally, for both healthy and depressed subjects, heart rate during interoception did not differ from the average heart rate during the task itself (p > .3), nor did heart rate during heartbeat interoception differ between subjects (t_{38} = .9, p = .36).

Focused Awareness Task Ratings

As previously described in the Methods section, subject responses were collected after half of the trials to help ensure subjects remained attentive to the task. Depressed and healthy subjects did not differ significantly in the reported subjective intensity of interoceptive sensations (see Table S1). The groups also did not differ in their accuracy in detecting exteroceptive targets (see Table S1), indicating that any observed group difference during the interoceptive attention condition is unlikely to be attributable to a global deficit in attention in the major depressive disorder (MDD) group.

Comorbidity within MDD Subjects

Nine of the MDD subjects had secondary comorbid anxiety disorders (social phobia n = 4, posttraumatic stress disorder n = 3, simple phobia n = 1, panic disorder n = 1). Depressed subjects with and without secondary comorbid anxiety diagnoses did not differ significantly in mean behavioral measures of anxiety or depression (HDRS: $t_{18} = .17$, p = .87; HARS: $t_{18} = .45$, p = .66; Table S7). Nor did the depressed subjects with or without comorbid anxiety disorders differ in activity of the dorsal mid-insula during heart interoception (left dorsal mid-insula: $t_{18} = -.18$, p = .86; right dorsal mid-insula: $t_{18} = -.32$, p = .75; Table S8).

We supplemented the ROI analyses mentioned above with whole-brain voxelwise analyses of the BOLD response during heart, stomach, and bladder interoception. After correction for multiple comparisons, we did not identify any regions of the brain exhibiting significant differences in response between depressed subjects with and without secondary comorbid anxiety diagnoses.

The Hemodynamic Response to Interoception and Other Behavioral Measures

We conducted further analyses of the relationship between the hemodynamic response during interoceptive attention and behavioral measures collected from healthy and depressed subjects.

Focused Awareness task ratings

The hemodynamic response within the dorsal mid-insula cortex (dmIC) during heartbeat interoception was significantly related to healthy subject's ratings of the intensity of heartbeat sensations (Right: r = -.73, p < .001; Left: r = -.47, p < .04), but not the ratings made by depressed subjects (Right: r = .24, p = .31; Left: r = .07, p = .78). A test of the difference in slopes of these relationships revealed that depressed and healthy subjects differed significantly in the relationship between right dmIC activity and heartbeat intensity ratings (t = -2.51, p < .02).

Subsequently, we conducted a whole-brain voxel-wise analysis to locate other brain regions exhibiting similar group differences in the relationship between heartbeat intensity ratings and BOLD response during heartbeat interoception. After correction for multiple comparisons, the right dmIC (Talairach coordinate: 38, -4, 11) was the only region of the brain that exhibited significant group differences in this relationship. The activation cluster within this group analysis was spatially contiguous with the right dmIC cluster where group differences in the magnitude of the hemodynamic response to heartbeat interoception were first observed (Figure 1).

Major depressive episode duration

ROI analysis results: We did not observe any significant correlations between dmIC task activation and major depressive episode duration in the depressed subjects (Table S9).

Somatic symptom severity

Voxel-wise analysis results: Depressed subjects exhibited a significant negative correlation between BOLD activity during heartbeat interoception and somatic symptom severity, as measured by the HDRS somatic symptom sub-scale (10), within bilateral amygdala and medial OFC (Table S10).

Anxiety severity

ROI analysis results: Within the depressed subjects, we observed no significant correlation between HARS scores and task activation within either dmlC cluster (Table S3).

Voxel-wise analysis results: After applying corrections for multiple comparisons, we did not observe any region of the brain that showed a significant relationship between activation during heartbeat interoception and anxiety, as measured by the HARS.

Additionally, using the AFNI program 3dttest++, we re-ran the whole-brain voxel-wise analysis of group differences in heartbeat interoception between depressed and healthy subjects (Figure 1, Table 2), this time including HARS severity scores as a covariate of no interest. The results of this analysis were almost identical to the results of the original analysis (e.g., see Figure 1, Table 2). All of the brain regions previously identified within this contrast were present after including the HARS covariate, though in some cases those regions were larger or smaller by a small number of voxels.

Functional Connectivity of the dmIC and Other Behavioral Measures

Somatic symptom severity

Depressed subjects exhibited a significant positive correlation between left dmIC functional connectivity and somatic symptom severity, as measured by the HDRS somatic symptom sub-scale (10), within right amygdala and right sgPFC (Table S11). After correction for multiple comparisons, no brain regions exhibited a significant correlation between right dmIC functional connectivity and somatic symptom severity. *Anxiety severity*

After applying corrections for multiple comparisons, we did not observe any region of the brain that showed a significant relationship between dmlC functional connectivity and anxiety, as measured by the HARS.

Additional Group Differences in Stomach and Bladder Interoception

Having identified that depressed subjects also exhibit decreased dmlC response to stomach and bladder interoception within the dmlC, we subsequently conducted

whole-brain group analyses comparing the hemodynamic response to stomach and bladder interoception between groups. The analyses were conducted as described in the methods section of the main paper, and both contrast maps were corrected for multiple comparisons as described above in the Supplemental Methods.

As expected, depressed subjects exhibited significantly decreased hemodynamic activity compared to healthy subjects within multiple other brain regions during attention to stomach and bladder sensations (Figure S5, Table S12), including many regions also observed within the heartbeat interoception contrast (Figure 1). Group differences in stomach and bladder interoception were observed in ventral mid-insula, a region previously identified along with dmIC as functionally selective for interoceptive attention, as well as the amygdala and OFC. Depressed subjects also exhibited decreased hemodynamic response within right dorsal anterior insula, involved in salience processing and focal attention (11; 12), as well as the right precuneus, a component of the default mode network (13), during stomach interoception.

Supplemental Discussion

Depression, Anxiety, and Interoceptive Awareness

Previous research suggests that both anxiety and depression play a part in modulating interoceptive awareness (14; 15). Some evidence suggests that anxiety and depression lie at opposite ends along a continuum of interoceptive awareness, with anxiety as a positive modulator and depression as a negative modulator (14). For example, trait anxiety has been associated with increased heartbeat perception accuracy (16) and panic disorder with increased sensitivity to anxiogenic challenge by sodium lactate infusion and 35% CO2 inhalation (17; 18). Depression, on the other hand, has been associated with decreased interoceptive accuracy and decreased heartbeat-evoked potential (14; 19).

However, due to the frequent comorbidity of mood and anxiety disorders (20), this relationship becomes much more complicated. The negative relationship between heartbeat perception accuracy and depression held only at high anxiety levels (14), and

depression-specific symptoms seem to modulate the relationship between anxiety and interoception (21). Additionally, though recent studies have attempted to account for this factor by recruiting depressed subjects with no comorbid anxiety disorders, those subjects still report significantly higher levels of anxiety than controls (22). One possible explanation for these discrepant findings comes from the hypothesis that, rather than considering anxiety and depression to be two distinct conditions, major depressive episodes occur as an adaptive, homeostatic response, possibly to chronically high levels of anxiety (23). In this scenario, the acute state of depression, with its accompanying physiological changes, such as decreased parasympathetic regulation of cardiac tone (24) and decreased baroreceptor sensitivity (25), conceivably may result in decreased interoceptive awareness, regardless of the presence of anxiety. However, this does not entirely preclude the effect of anxiety, as higher levels of chronic anxiety conceivably may lead to more severe depression and thus result in a greater decrease in interoceptive awareness.

In this study, depressed subjects both with and without comorbid anxiety disorders had significantly higher levels of both anxiety and depressive symptoms than controls, accompanied by significantly decreased dmIC activation during interoceptive attention. Within MDD subjects, severity of depression (as rated by the HDRS scores) negatively correlated with activation during heartbeat interoception within the insula, as well as with resting state functional connectivity between the insula and depression-associated brain regions. A subsequent analysis using sub-scales of the HDRS (10) revealed that the relationship between heartbeat interoception and depression severity was strongly driven by the severity of somatic symptoms in depressed subjects. Importantly, behavioral measures of anxiety alone did not significantly modulate heartbeat interoception; neither did the presence of comorbid anxiety disorders among the MDD subjects. This suggests that, within these subjects, the hemodynamic activity within the insula during visceral interoception is most strongly associated with the somatic symptoms that accompany major depression.

The Focused Awareness Task

The Focused Awareness task originally was designed to identify areas of the insula selectively responsive for cognitive, sensory, and emotional processes, in an attempt to reconcile patterns of activation reported across various studies that overlap within the same regions of the insula. Neuroimaging studies of gustation (a sensory modality that shares a common neural pathway with vagal afferents from the heart and viscera (26)) also frequently report a variability in the location of gustatory activation within the insula, dependent on the specific cognitive requirements of the task (27; 28). The Focused Awareness task thus was designed so that participants would passively attend to the sensations from their heart and viscera, in order to directly isolate primary viscerosensory regions of the insula, without the confounding demands of other cognitive tasks, such as exteroceptive attention to compare heartbeats against external auditory tones. The results of the Focused Awareness task bear this out, as attention to heart and stomach sensations selectively activated regions of the mid-insula identified through cytoarchitecture, anatomical studies, and neuroimaging meta-analyses as primary viscerosensory areas of the insula (26; 29-32).

Through this method, we are able to identify group differences in activation during interoceptive *attention* within these primary sensory regions of the insula, though the very nature of the task precludes the ability to identify group differences in interoceptive *accuracy*. Within the current study, the self-report ratings made by subjects after interoceptive attention trials relate specifically to the subjective intensity of their experience during the preceding trial, and were primarily included to ensure that subjects remained attentive to the task. Our comparisons of intensity ratings between groups were done in order to confirm that both depressed and healthy subjects performed the task equivalently. Given that these ratings were not measures of objective interoceptive accuracy, the lack of group differences in the magnitude of these ratings does not noticeably contradict findings from previous studies measuring heartbeat perception accuracy in depression (19; 22; 33; 34).

The lack of an external accuracy measure for interoceptive trials makes it difficult to verify objectively that all subjects performed the task equivalently. However, analysis of post-trial rating periods, during which subjects reported the subjective intensity of

interoceptive sensations or the number of targets presented, allows us to demonstrate that the two groups performed the exteroception tasks equally well and rated the interoceptive sensations as having equal intensity (see Supplemental Results section). In post-scan interviews, all MDD and healthy control subjects reported both understanding and performing the interoception task.

Additionally, we have demonstrated in a separate study that the accuracy of subjects' interoceptive perceptions is correlated with the activity of the mid-insula during this same interoception task used in the present study (35). This gives us even more confidence that MDD participants are performing the interoception task as instructed, and that the activity of this region is related to interoceptive awareness.

Analysis of the Focused Awareness task data within this study revealed group differences within a specific region of the insula, previously identified as selective for visceral interoception. In depressed subjects, activity within this region during heartbeat interoception was correlated with the severity of their depression (r = -.44; p = .05) as well as the severity of their somatic symptoms (r = -.53; p = .02). Likewise, in depressed subjects, the functional connectivity between this region and limbic brain regions such as the amygdala also correlated with depression severity (Figure S3). These findings all indicate that the results of this study accurately reflect depression-related effects on the cortical representation of visceral interoception.

Table S1. Focused Awareness task ratings

| | HC Mean (SD) | MDD Mean (SD) | t ₃₈ | p | | | | | |
|---------------------------|--------------|---------------|------------------------|-----|--|--|--|--|--|
| Intensity Rating | S | | | | | | | | |
| Heart | 4.08 (1.75) | 4.31 (1.50) | 45 | .66 | | | | | |
| Stomach | 4.6 (1.57) | 4.88 (1.50) | 58 | .56 | | | | | |
| Bladder | 5.06 (1.66) | 4.29 (1.81) | 1.40 | .17 | | | | | |
| Target Detection Accuracy | | | | | | | | | |
| % Accuracy | 90.0 (15.7) | 85.5 (13.5) | .96 | .34 | | | | | |

HC, healthy controls; MDD, major depressive disorder subjects.

Table S2. Group differences in dmlC activity during stomach and bladder interoception

| | Healthy Subjects | | | MDD \$ | MDD Subjects | | HC-I | MDD |
|---------|------------------|------------------------|-------|------------|------------------------|-----|------------------------|------|
| | % sign | % signal change | | | al chan | ge | | |
| | Mean (SD) | t ₁₉ | р | Mean (SD) | t ₁₉ | р | <i>t</i> ₃₈ | р |
| L dmIC | | | | | | | | |
| Stomach | .028 (.02) | 7.26 | <.001 | .010 (.02) | 2.17 | .04 | 2.99 | .005 |
| Bladder | .023 (.02) | 4.59 | <.001 | .005 (.02) | .84 | .41 | 2.52 | .02 |
| R dmlC | | | | | | | | |
| Stomach | .031 (.02) | 6.99 | <.001 | .014 (.03) | 2.00 | .06 | 1.99 | .05 |
| Bladder | .029 (.03) | 3.87 | .001 | .008 (.03) | 1.06 | .30 | 1.97 | .06 |

dmIC, dorsal mid-insula cortex; HC, healthy controls; L, left; MDD, major depressive disorder subjects; R, right.

Table S3. Correlation of dmlC activity during interoception with total HDRS and HARS rating scale scores in the depressed subjects

| | HD | RS | HAF | RS |
|---------|------------------------|-----|------------------------|-----|
| | <i>r</i> ₁₈ | p | <i>r</i> ₁₈ | p |
| L dmIC | | | | |
| Heart | 44 | .05 | 23 | .33 |
| Stomach | 18 | .45 | 13 | .58 |
| Bladder | 31 | .18 | 27 | .26 |
| | | | | |
| R dmIC | | | | |
| Heart | 31 | .18 | 10 | .68 |
| Stomach | .14 | .56 | 02 | .94 |
| Bladder | 03 | .92 | 12 | .62 |

dmIC, dorsal mid-insula cortex; HARS, Hamilton Anxiety Rating Scale; HDRS, Hamilton Depression Rating Scale; L, left; MDD, major depressive disorder subjects; R, right.

Table S4. Correlation of dmlC activity during heartbeat interoception with HDRS sub-scales in depressed subjects from (Cleary and Guy, (10))

| | L dmIC | | R di | mIC |
|--------------------------|------------------------|-----|------------------------|------|
| HDRS Factor | <i>r</i> ₁₈ | р | r ₁₈ | р |
| Anxiety/Somatization | 53 | .02 | 41 | .07 |
| Weight Loss ^a | | | | |
| Cognitive Disturbance | .03 | .90 | <.01 | >.99 |
| Diurnal Variation | .03 | .90 | 12 | .61 |
| Retardation | 13 | .59 | 03 | .89 |
| Sleep Disturbance | 06 | .81 | 01 | .95 |

^a The Weight Loss factor from Cleary and Guy (10) was excluded as no subjects reported significant weight changes.

Bolded values indicate significance.

dmIC, dorsal mid-insula cortex; HDRS, Hamilton Depression Rating Scale; L, left; R, right.

Table S5. Brain regions where the hemodynamic response to heartbeat interoception was correlated with depression severity^a

| Side / Location | Peak | Coordin | nates ^b | <i>t</i> ₃₈ | Volume |
|---------------------------------------|------|---------|--------------------|------------------------|--------|
| | Х | Υ | Z | | (mm³) |
| L Amygdala | -25 | -4 | -19 | -4.54 | 1549 |
| L Ventral Anterior Insula | -36 | +10 | -7 | -5.58 | 1184 |
| L Posterior OFC (BA13a) | -10 | +13 | -10 | -4.69 | 997 |
| L Superior Parietal Lobule | -24 | -55 | +39 | -6.90 | 590 |
| L Middle Occipital Gyrus ^c | -29 | -69 | +21 | -5.45 | 557 |
| L Ventral and Dorsal Mid-Insula | -36 | -4 | 2 | -3.60 | 214 |
| R Amygdala | +18 | +1 | -17 | -3.44 | 107 |

^a Within the depressed subjects.

BA, Brodmann area; L, left; OFC, orbitofrontal cortex; R, right.

^b All coordinates reported according to Talairach stereotaxic atlas (1). This format uses three numbers (X,Y,Z) to describe the distance from the anterior commissure. The X,Y,Z dimensions refer to right(+)-to-left(-), anterior(+)-to-posterior(-), and dorsal(+)-to-ventral(-) respectively.

Table S6. Brain regions where functional connectivity with the dmlC was correlated with depression severity

| Side / Location | Peak (| Coordin | ates ^a | <i>t</i> ₁₈ | Volume |
|----------------------------|--------|---------|-------------------|------------------------|--------|
| | X | Υ | Z | | (mm³) |
| Left dmIC Seed | | | | | |
| R Posterior OFC (BA13a) | +10 | +22 | -8 | 4.94 | 879 |
| R Subgenual PFC (BA32pl) | | | | | |
| R Medial OFC (BA11l/m) | +22 | +55 | -8 | 4.60 | 573 |
| L Ventral Mid-Insula | -39 | -3 | -14 | 4.79 | 498 |
| L Posterior OFC (BA13a) | -8 | +17 | -12 | 4.69 | 466 |
| L Subgenual PFC (BA32pl) | | | | | |
| R Supramarginal Gyrus | +34 | -52 | +27 | 5.99 | 391 |
| R Ventral Posterior Insula | -38 | -19 | +2 | 3.86 | 381 |
| L Middle Temporal Gyrus | -52 | -40 | -3 | 5.13 | 279 |
| L Amygdala | -18 | +4 | -14 | 3.63 | 166 |
| L Medial OFC (BA11I/m) | -15 | +52 | -10 | 4.26 | 150 |
| Right dmIC Seed | | | | | |
| R Ventral Anterior Insula | +36 | +11 | -5 | 5.04 | 1201 |
| R Medial OFC (BA11I/m) | +22 | +48 | -7 | 5.34 | 1120 |
| L Posterior OFC (BA13a) | -18 | +8 | -12 | 4.71 | 900 |
| R Inferior Frontal Gyrus | +46 | +22 | +13 | 6.13 | 718 |
| L Ventral Mid-Insula | -36 | -1 | -12 | 4.30 | 488 |
| R Ventral Posterior Insula | -38 | -15 | -1 | 4.14 | 343 |
| R Superior Frontal Gyrus | +20 | +52 | +25 | 4.96 | 241 |
| L Ventral Anterior Insula | -34 | +15 | -1 | 4.03 | 230 |
| L Subgenual PFC (BA32pl) | -4 | +20 | -12 | 4.00 | 204 |
| L Medial OFC (BA11I/m) | -20 | +39 | -12 | 3.87 | 123 |
| R Posterior OFC (BA13a) | +13 | +18 | -17 | 3.26 | 113 |
| L Medial OFC (BA11I/m) | -13 | +52 | -8 | 3.76 | 86 |

^a All coordinates reported according to Talairach stereotaxic atlas (1). This format uses three numbers (X,Y,Z) to describe the distance from the anterior commissure. The X,Y,Z dimensions refer to right(+)-to-left(-), anterior(+)-to-posterior(-), and dorsal(+)-to-ventral(-) respectively.

BA, Brodmann area; dmIC, dorsal mid-insula cortex; L, left; OFC, orbitofrontal cortex; PFC, prefrontal cortex; R, right.

Table S7. Comparison of MDD subjects with and without secondary comorbid anxiety diagnoses

| Demographics | | | | | | | | |
|--------------|------------------|-----------------|------------------------|-----------------|--|--|--|--|
| | MDD w/o comorbid | MDD w/ comorbid | <i>t</i> ₁₈ | <i>p</i> -value | | | | |
| HDRS | 23.6 (7.9) | 23.0 (8.8) | .17 | .87 | | | | |
| HARS | 17.5 (5.3) | 16.4 (4.4) | .45 | .66 | | | | |

HARS, Hamilton Anxiety Rating Scale; HDRS, Hamilton Depression Rating Scale; MDD, major depressive disorder subjects; w/, with; w/o, without.

Table S8. Comparison of dmlC activity during heartbeat interoception between MDD subjects with and without comorbid anxiety disorders

| | MDD w/o comorbid % signal change | | | | MDD w/ comorbid % signal change | | | -MDD _{w/} |
|--------|-------------------------------------|------------------------|-----|------------|------------------------------------|-----|------------------------|--------------------|
| | Mean (SD) | <i>t</i> ₁₀ | р | Mean (SD) | <i>t</i> ₈ | р | <i>t</i> ₁₈ | р |
| L dmIC | 0004 (.03) | 04 | .97 | 003 (.03) | 27 | .79 | .18 | .86 |
| R dmIC | 002 (.04) | 15 | .88 | .003 (.03) | .31 | .76 | 32 | .75 |

dmIC, dorsal mid-insula cortex; L, left; MDD, major depressive disorder subjects; R, right; w/, with; w/o, without.

Table S9. Correlation of dmIC activity during interoception with MDE duration in the depressed subjects

| | L dmlC | | R dr | nIC |
|---------|--------|-----|------------------------|-----|
| | | | r ₁₈ | p |
| Heart | -0.13 | .60 | -0.12 | .60 |
| Stomach | 0.21 | .38 | 0.12 | .60 |
| Bladder | 0.22 | .36 | 0.15 | .51 |

dmIC, dorsal mid-insula cortex; L, left; MDE, major depressive episode; R, right.

Table S10. Brain regions where the hemodynamic response to heartbeat interoception was correlated with somatic symptom severity^a

| Side / Location | nates ^b | <i>t</i> ₁₈ | Volume | | |
|----------------------|--------------------|------------------------|--------|-------|-------|
| | X | Υ | Z | | (mm³) |
| R Amygdala | +18 | -1 | -17 | -3.60 | 140 |
| R Medial OFC (BA11m) | +11 | +25 | -12 | -3.87 | 140 |
| L Amygdala | +18 | +1 | -17 | -3.44 | 118 |

^a Within the depressed subjects, assessed by the somatic subscale of the HDRS, developed by Cleary and Guy (10).

Table S11. Brain regions where functional connectivity with the dmIC was correlated with somatic symptom severity^a

| Side / Location | Peak | Coordin | ates ^b | <i>t</i> ₁₈ | Volume |
|--------------------------|------|---------|-------------------|------------------------|--------|
| | X | Υ | Z | | (mm³) |
| Left dmIC Seed | | | | | |
| R Amygdala | +22 | -1 | -24 | 4.68 | 118 |
| R Subgenual PFC (BA32pl) | +4 | +15 | -14 | 4.26 | 102 |

^a Within the depressed subjects, assessed by the somatic subscale of the HDRS, developed by Cleary and Guy (10).

^b All coordinates reported according to Talairach stereotaxic atlas (1). This format uses three numbers (X,Y,Z) to describe the distance from the anterior commissure. The X,Y,Z dimensions refer to right(+)-to-left(-), anterior(+)-to-posterior(-), and dorsal(+)-to-ventral(-) respectively.

BA, Brodmann area; HDRS, Hamilton Depression Rating Scale; L, left; OFC, orbitofrontal cortex; R, right.

^b All coordinates reported according to Talairach stereotaxic atlas (1). This format uses three numbers (X,Y,Z) to describe the distance from the anterior commissure. The X,Y,Z dimensions refer to right(+)-to-left(-), anterior(+)-to-posterior(-), and dorsal(+)-to-ventral(-) respectively.

BA, Brodmann area; dmIC, dorsal mid-insula cortex; HDRS, Hamilton Depression Rating Scale; PFC, prefrontal cortex; R, right.

Table S12. Brain regions exhibiting differences in the hemodynamic response to stomach and bladder interoception between healthy and depressed subjects^a

| Side / Location | Peak | Coordii | nates ^b | <i>t</i> ₁₈ | Volume |
|--------------------------------------|------|---------|--------------------|------------------------|--------|
| | Х | Υ | Z | | (mm³) |
| Bladder Interoception | | | | | |
| R Claustrum | +36 | -10 | -1 | 3.70 | 162 |
| R Putamen | | | | | |
| R Lateral OFC (BA11I) | +22 | +32 | -10 | 3.70 | 123 |
| R Ventral Mid-Insula | +48 | +2 | -3 | 3.46 | 86 |
| R Posterior OFC (BA13a) | +20 | +13 | -15 | 4.59 | 45 |
| R Amygdala | +20 | -1 | -10 | 3.52 | 42 |
| Stomach Interoception | | | | | |
| Right OFC (BA11/13) | +16 | +32 | -10 | 5.17 | 6287 |
| Left Superior Parietal Lobule | -29 | -50 | +42 | 5.09 | 1410 |
| Left Middle Occipital Gyrus | -48 | -66 | -3 | 4.53 | 1088 |
| Right Precuneus | +6 | -64 | +46 | 4.64 | 874 |
| Right Cerebellum | -6 | -76 | -17 | 4.67 | 858 |
| Left Precentral Gyrus | -17 | -8 | +44 | 4.83 | 831 |
| Left Ventral Anterior and Mid Insula | -38 | +6 | -3 | 4.81 | 670 |
| Right Ventral Mid Insula | +36 | +4 | -7 | 4.22 | 665 |
| Left Inferior Parietal Lobule | -50 | -29 | +37 | 4.56 | 638 |
| Right Mid Cingulate Gyrus | +11 | -15 | +30 | 5.20 | 616 |
| Right Claustrum | +34 | -17 | +0 | 4.33 | 391 |
| Right Dorsal Anterior Insula | +36 | +22 | +6 | 3.68 | 370 |
| Left Amygdala | | | | | |

BA, Brodmann area; MDD, major depressive disorder; OFC, orbitofrontal cortex; R, right.

^a In all cases, activity was greater in healthy subjects compared to the MDD group.
^b All coordinates reported according to Talairach stereotaxic atlas (1). This format uses three numbers (X,Y,Z) to describe the distance from the anterior commissure. The X,Y,Z dimensions refer to right(+)to-left(-), anterior(+)-to-posterior(-), and dorsal(+)-to-ventral(-) respectively.

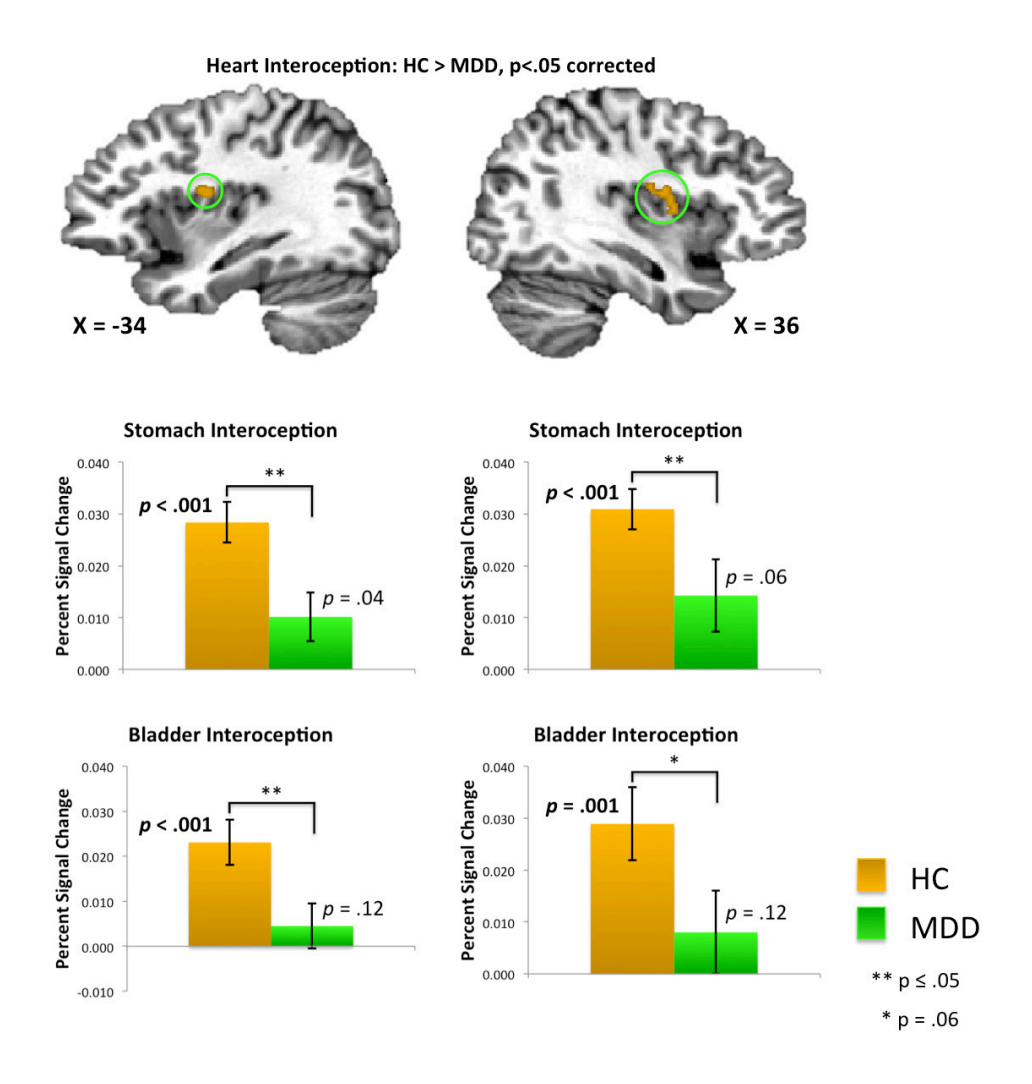


Figure S1. Group differences in stomach and bladder Interoception. Healthy participants (yellow bar) exhibited significantly greater activation within the dmIC ROIs – which were identified in the heartbeat interoception contrast (Figure 1) - during stomach and bladder interoception than during the exteroceptive control condition. In most cases, the depressed participants (green bar) exhibited reliably less activation during stomach and bladder interoception than the healthy subjects. Importantly, within this region of the insula, healthy and depressed subjects did not differ in activation during the exteroceptive control condition (Left ROI: p = 0.18, Right ROI: p = 0.23). HC, healthy controls; MDD, major depressive disorder subjects.

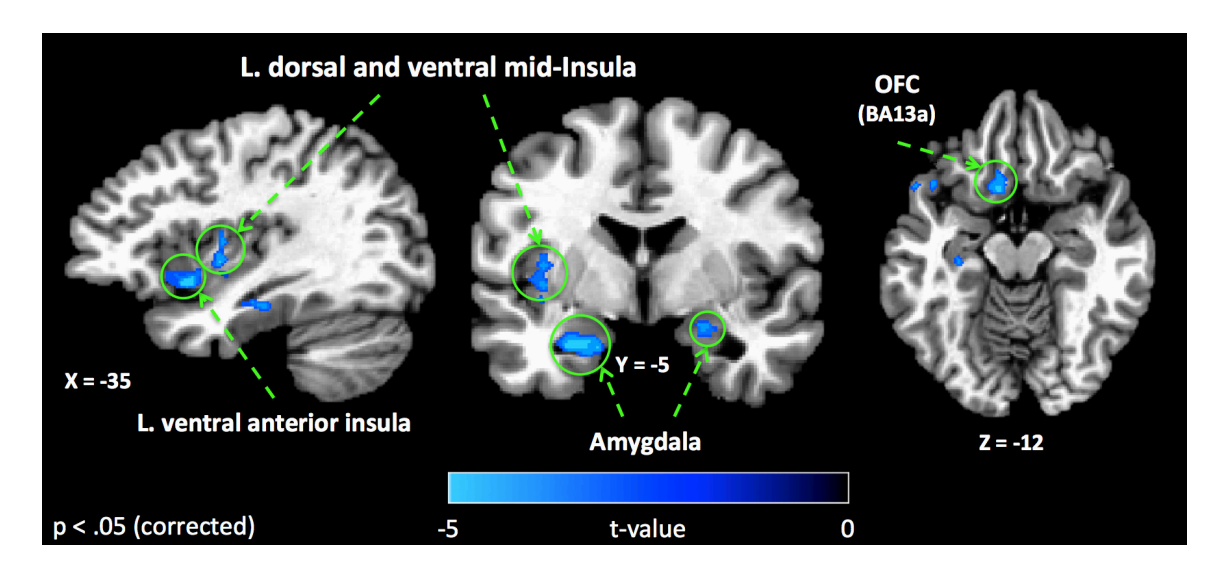


Figure S2. Brain regions where activation during heartbeat interoception is correlated with depression severity. Depressed subjects exhibited a significant negative correlation between hemodynamic activity during heartbeat interoception and scores on the Hamilton Depression Rating Scale within left ventral anterior and ventral and dorsal mid-insula, as well as right posterior OFC and bilateral amygdala. All results shown were corrected for multiple comparisons at $p_{corrected} < .05$. BA, Brodmann area; L., left; OFC, orbitofrontal cortex.

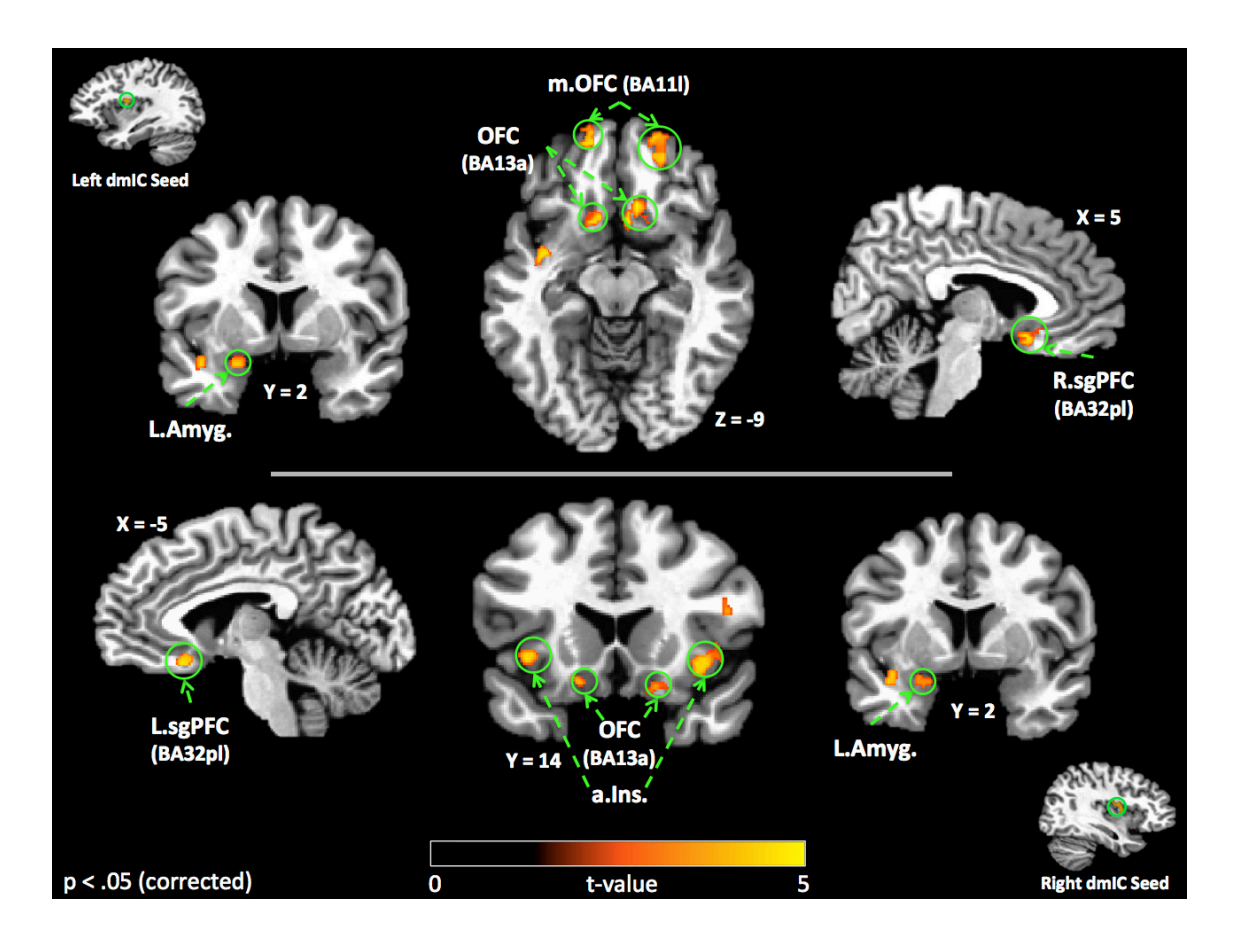


Figure S3. Dorsal mid-insula resting-state functional connectivity is correlated with depression severity. This figure shows the brain regions where resting-state functional connectivity to the dmlC was significantly correlated with depression severity. Many of these regions, notably the left amygdala and regions of the orbitofrontal cortex, also exhibited significant group differences in functional connectivity to the dmlC (see Figure 3). All results corrected for multiple comparisons at $p_{corrected} < .05$. a.Ins., anterior insula; Amyg., amygdala; BA, Brodmann area; dmlC, dorsal mid-insula cortex; L., left; m., medial; OFC, orbitofrontal cortex; R., right; sgPFC, subgenual prefrontal cortex.

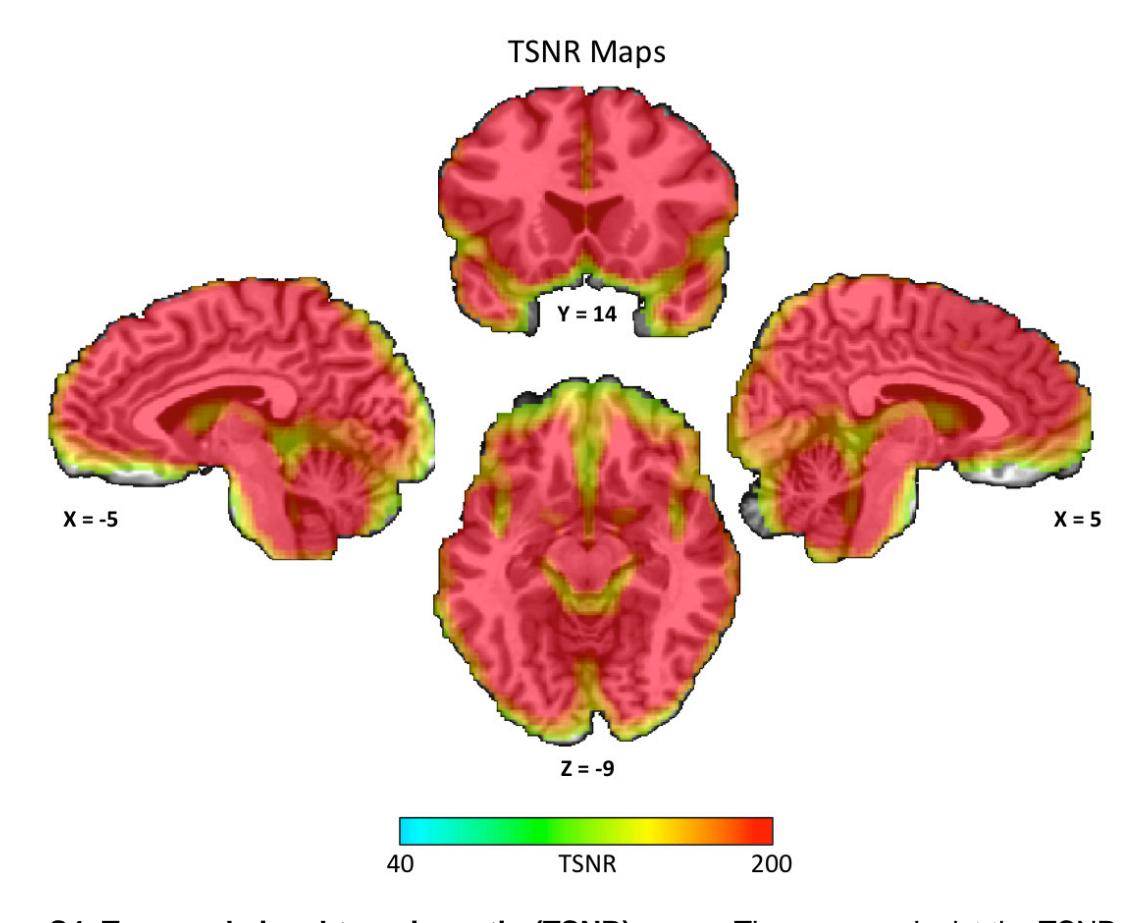


Figure S4. Temporal signal-to-noise ratio (TSNR) maps. These maps depict the TSNR of the smoothed echo-planar imaging time course data acquired in this study. TSNR was calculated by dividing each voxel's mean signal intensity by the standard deviation of the residual time-course, obtained by subtracting the regression model from the signal time-course. All colored areas shown have TSNR of at least 40, the minimum to reliably detect effects between conditions in fMRI data (7). All the figures in this text are displayed strictly within a mask where TSNR > 40.

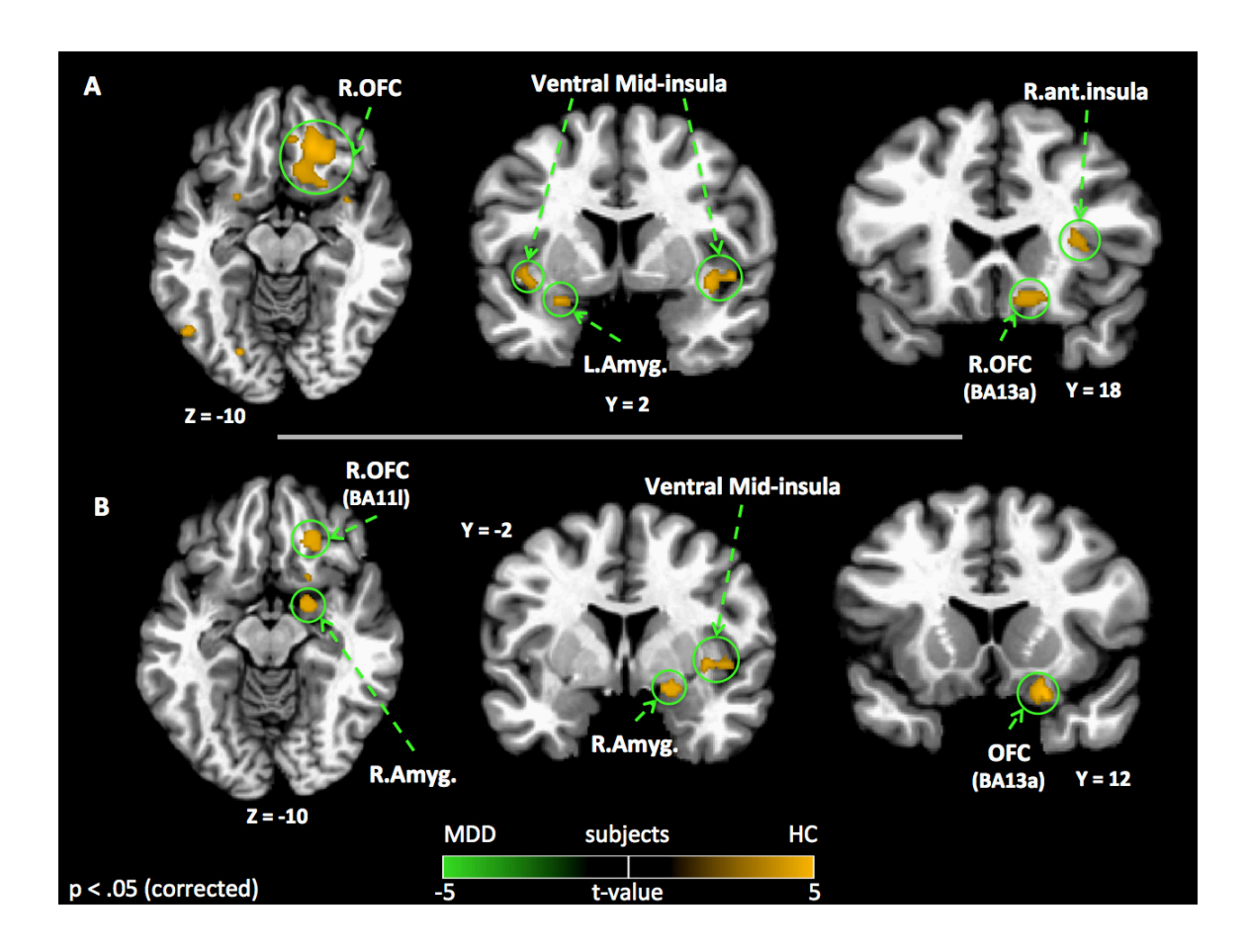


Figure S5. Group differences in stomach and bladder interoception. Outside of the dmlC, depressed subjects exhibited decreased hemodynamic activity compared to healthy subjects within multiple other brain regions during attention to stomach and bladder sensations (**A**: Stomach Interoception, **B**: Bladder Interoception). Group differences in stomach and bladder interoception were observed in ventral mid-insula and right OFC, as well as right and left amygdala. Depressed subjects also exhibited decreased hemodynamic response within right dorsal anterior insula during stomach interoception. All results shown were corrected for multiple comparisons at $p_{corrected} < .05$. Amyg., amygdala; ant., anterior; BA, Brodmann area; dmlC, dorsal mid-insula cortex; HC, healthy controls; L, left; MDD, major depressive disorder subjects; OFC, orbitofrontal cortex; R., right.

Supplemental References

- 1. Talairach J, Tournoux JTP (1988): *Co-planar Stereotaxic Atlas of the Human Brain*. New York: Thieme Medical Publishers.
- 2. Jo HJ, Saad ZS, Simmons WK, Milbury LA, Cox RW (2010): Mapping sources of correlation in resting state FMRI, with artifact detection and removal. *Neuroimage* 52: 571–582.
- 3. Glover GH, Li T-Q, Ress D (2000): Image-based method for retrospective correction of physiological motion effects in fMRI: RETROICOR. *Magn Reson Med* 44: 162–167.
- 4. Birn RM, Murphy K, Bandettini PA (2008): The effect of respiration variations on independent component analysis results of resting state functional connectivity. *Hum Brain Mapp* 29: 740–750.
- 5. Power JD, Barnes KA, Snyder AZ, Schlaggar BL, Petersen SE (2012): Spurious but systematic correlations in functional connectivity MRI networks arise from subject motion. *Neuroimage* 59: 2142–2154.
- 6. Saad ZS, Gotts SJ, Murphy K, Chen G, Jo HJ, Martin A, Cox RW (2012): Trouble at rest: how correlation patterns and group differences become distorted after global signal regression. *Brain Connect* 2: 25–32.
- 7. Murphy K, Bodurka J, Bandettini PA (2007): How long to scan? The relationship between fMRI temporal signal to noise ratio and necessary scan duration. *Neuroimage* 34: 565–574.
- 8. Desikan RS, Ségonne F, Fischl B, Quinn BT, Dickerson BC, Blacker D, *et al.* (2006): An automated labeling system for subdividing the human cerebral cortex on MRI scans into gyral based regions of interest. *Neuroimage* 31: 968–980.
- 9. Chiavaras MM, Legoualher G, Evans A, Petrides M (2001): Three-dimensional probabilistic atlas of the human orbitofrontal sulci in standardized stereotaxic space. *Neuroimage* 13: 479–496.
- 10. Cleary P, Guy W (1977): Factor analysis of the Hamilton depression scale. *Drugs Exp Clin Res* 1: 115–120.
- 11. Bud Craig AD (2009): How do you feel now? The anterior insula and human awareness. *Nat Rev Neurosci* 10: 59–70.
- 12. Nelson SM, Dosenbach NUF, Cohen AL, Wheeler ME, Schlaggar BL, Petersen SE (2010): Role of the anterior insula in task-level control and focal attention. *Brain Struct Funct* 214: 669–680.

- 13. Li B, Liu L, Friston KJ, Shen H, Wang L, Zeng L-L, Hu D (2013): A treatment-resistant default mode subnetwork in major depression. *Biol Psychiatry* 74: 48–54.
- 14. Pollatos O, Traut-Mattausch E, Schandry R (2009): Differential effects of anxiety and depression on interoceptive accuracy. *Depress Anxiety* 26: 167–173.
- 15. Paulus MP, Stein MB (2010): Interoception in anxiety and depression. *Brain Struct Funct* 214: 451–463.
- 16. Domschke K, Stevens S, Pfleiderer B, Gerlach AL (2010): Interoceptive sensitivity in anxiety and anxiety disorders: An overview and integration of neurobiological findings. *Clin Psychology Rev* 30: 1–11.
- 17. Johnson PL, Truitt W, Fitz SD, Minick PE, Dietrich A, Sanghani S, *et al.* (2010): A key role for orexin in panic anxiety. *Nat Med* 16: 111–115.
- 18. Perna G, Barbini B, Cocchi S, Bertani A, Gasperini M (1995): 35% CO2 challenge in panic and mood disorders. *J Affect Disord* 33: 189–194.
- 19. Terhaar J, Viola FC, Bär K-J, Debener S (2012): Heartbeat evoked potentials mirror altered body perception in depressed patients. *Clin Neurophysiol* 123: 1950–1957.
- 20. Gorman JM (1996): Comorbid depression and anxiety spectrum disorders. *Depress Anxiety* 4: 160–168.
- 21. Dunn BD, Stefanovitch I, Evans D, Oliver C, Hawkins A, Dalgleish T (2010): Can you feel the beat? Interoceptive awareness is an interactive function of anxiety- and depression-specific symptom dimensions. *Behav Res Ther* 48: 1133–1138.
- 22. Furman DJ, Waugh CE, Bhattacharjee K, Thompson RJ, Gotlib IH (2013): Interoceptive awareness, positive affect, and decision making in Major Depressive Disorder. *J Affect Disord* 151: 780–785.
- 23. Andrews PW, Kornstein SG, Halberstadt LJ, Gardner CO, Neale MC (2011): Blue again: perturbational effects of antidepressants suggest monoaminergic homeostasis in major depression. *Front Psychol* 2: 159.
- 24. Carney RM, Blumenthal JA, Freedland KE, Stein PK, Howells WB, Berkman LF, *et al.* (2005): Low heart rate variability and the effect of depression on post-myocardial infarction mortality. *Arch Intern Med* 165: 1486–1491.
- 25. Broadley AJM, Frenneaux MP, Moskvina V, Jones CJH, Korszun A (2005): Baroreflex sensitivity is reduced in depression. *Psychosom Med* 67: 648–651.
- 26. Craig AD (2002): How do you feel? Interoception: the sense of the physiological condition of the body. *Nat Rev Neurosci* 3: 655–666.

- 27. Small DM (2010): Taste representation in the human insula. *Brain Struct Funct* 214: 551–561.
- 28. Veldhuizen MG, Albrecht J, Zelano C, Boesveldt S, Breslin P, Lundström JN (2011): Identification of human gustatory cortex by activation likelihood estimation. *Hum Brain Mapp* 32: 2256–2266.
- 29. Morel A, Gallay MN, Baechler A, Wyss M, Gallay DS (2013): The human insula: Architectonic organization and postmortem MRI registration. *Neuroscience* 236: 117–135.
- 30. Proserpio P, Cossu M, Francione S, Tassi L, Mai R, Didato G, *et al.* (2011): Insular-opercular seizures manifesting with sleep-related paroxysmal motor behaviors: a stereo-EEG study. *Epilepsia* 52: 1781–1791.
- 31. Kurth F, Zilles K, Fox PT, Laird AR, Eickhoff SB (2010): A link between the systems: functional differentiation and integration within the human insula revealed by meta-analysis. *Brain Struct Funct* 214: 519–534.
- 32. Kelly C, Toro R, Di Martino A, Cox CL, Bellec P, Castellanos FX, Milham MP (2012): A convergent functional architecture of the insula emerges across imaging modalities. *Neuroimage* 61: 1129–1142.
- 33. Dunn BD, Dalgleish T, Ogilvie AD, Lawrence AD (2007): Heartbeat perception in depression. *Behav Res Ther* 45: 1921–1930.
- 34. Mussgay L, Klinkenberg N, Rüddel H (1999): Heart beat perception in patients with depressive, somatoform, and personality disorders. *J Psychophysiol* 13: 27–36.
- 35. Kleckner IR, Avery JA, Quigley KS, Simmons WK, Barrett LF (2013, October 28): Neural correlates of interoceptive attention and interoceptive accuracy. *Cognitive Neuroscience Society.* San Francisco, CA.